ASTROGEOLOGIC STUDIES

ANNUAL PROGRESS REPORT

October 1, 1968 to September 30, 1969

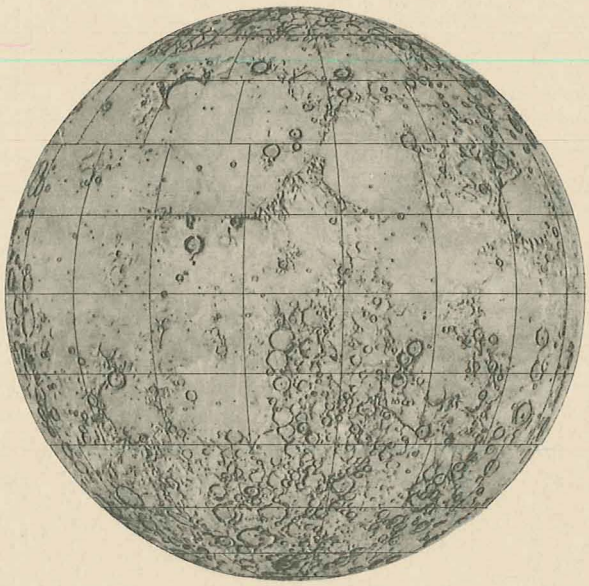

DEPARTMENT OF THE INTERIOR

UNITED STATES GEOLOGICAL SURVEY

ASTROGEOLOGIC STUDIES
ANNUAL PROGRESS REPORT

October 1, 1968 to
September 30, 1969

January 1970

This preliminary report is distributed without editorial and technical review for conformity with official standards and nomenclature. It should not be quoted without permission.

This report concerns work done on behalf of the National Aeronautics and Space Administration.

DEPARTMENT OF THE INTERIOR
UNITED STATES GEOLOGICAL SURVEY

CONTENTS

DISTRIBUTION

	No. of Copies
National Aeronautics and Space Administration Washington, D. C.	20
U. S. Geological Survey	10
Abelson, Dr. P. H., Director Geophysical Laboratory Carnegie Institution Washington, D. C.	1
Adler, Mr. Isidore Goddard Space Flight Center Greenbelt, Maryland	1
Allen, Mr. H. J. Ames Research Center National Aeronautics and Space Administration Moffett Field, California	1
Allenby, Dr. R. J. Assistant Director of Lunar Science Office of Manned Space Flight National Aeronautics and Space Administration Washington, D. C.	1
Babcock, Dr. H. W., Director Mt. Wilson and Palomar Observatories Mount Wilson, California	1
Barringer, Mr. R. W. The Barringer Crater Company The Regency Apartments St. Davids, Pennsylvania	1
Beattie, Mr. D. A. Office of Manned Space Flight National Aeronautics and Space Administration Washington, D. C.	1
Bellcomm Technical Library Washington, D. C.	1

DISTRIBUTION--Continued

	No. of Copies
Billingham, Mr. John Biotechnology Division Ames Research Center Moffett Field, California	1
Brett, Dr. P. R., Chief Geochemistry Branch Manned Spacecraft Center National Aeronautics and Space Administration Houston, Texas	1
Broome, Mr. Calvin Viking Project Office Langley Research Center Hampton, Virginia	1
Burcham, Dr. D. P. Space Science Division Jet Propulsion Laboratory California Institute of Technology Pasadena, California	1
Burke, Mr. J. D. Jet Propulsion Laboratory California Institute of Technology Pasadena, California	1
Bryson, Mr. R. P. Office of Manned Space Flight National Aeronautics and Space Administration Washington, D. C.	2
Calio, Mr. Anthony Manned Spacecraft Center National Aeronautics and Space Administration Houston, Texas	1
Carder, Mr. R. W. Aeronautical Chart and Information Center St. Louis, Missouri	1
Carlile, Mr. C. D. Marshall Space Flight Center Huntsville, Alabama	1

	No. of Copies
Casey, Mr. J. N. Assistant Director for Geology Bureau of Mineral Resources P. O. Box 378 Canberra, Australia	1
Center for Radiophysics and Space Research Cornell University Space Sciences Building Ithaca, New York	1
Chapman, Dr. D. R. Ames Research Center National Aeronautics and Space Administration Moffett Field, California	1
Clark, Dr. J. F. Goddard Space Flight Center Greenbelt, Maryland	1
Cortright, Mr. E. M., Director Langley Research Center Hampton, Virginia	1
Costes, Dr. N. C. Marshall Space Flight Center Huntsville, Alabama	1
Davin, Mr. E. M. National Aeronautics and Space Administration Washington, D. C.	1
Deutsch, Dr. Stanley National Aeronautics and Space Administration Washington, D. C.	1
Dollfus, Dr. Audouin Observatoire de Paris Meudon, France	1
Dominion Observatory, Director Ottawa, Ontario Canada	1

DISTRIBUTION--Continued

	No. of Copies
Dornbach, Dr. J. E. Earth Resources Division Manned Spacecraft Center National Aeronautics and Space Administration Houston, Texas	1
Downey, Mr. J. A. Marshall Space Flight Center Huntsville, Alabama	1
Dwornik, Mr. S. E. Planetology Chief Office of Space Science and Applications National Aeronautics and Space Administration Washington, D. C.	1
El-Baz, Dr. Farouk Bellcomm, Inc. Washington, D. C.	1
Faget, Mr. Maxime Manned Spacecraft Center National Aeronautics and Space Administration Houston, Texas	1
Fielder, Dr. Gilbert University of London Observatory London England	1
Fordyce, Mr. S. W. National Aeronautics and Space Administration Washington, D. C.	1
Foss, Dr. T. H. Manned Spacecraft Center National Aeronautics and Space Administration Houston, Texas	1
Foster, Mr. W. B. National Aeronautics and Space Administration Washington, D. C.	1
Fredrick, Professor Laurence, Director Leander McCormick Observatory University of Virginia Charlottesville, Virginia	1

	No. of Copies
Freeberg, Mrs. J. H. U. S. Geological Survey Menlo Park, California	1
French, Mr. Bevan Goddard Space Flight Center Greenbelt, Maryland	1
Fuchs, Mr. R. A., Program Manager Advanced Lunar Projects Laboratory Hughes Aircraft Company El Segundo, California	1
Gault, Mr. D. E. Ames Research Center National Aeronautics and Space Administration Moffett Field, California	1
Gill, Mr. M. R. National Aeronautics and Space Administration Washington, D. C.	1
Gilruth, Dr. R. R., Director Manned Spacecraft Center National Aeronautics and Space Administration Houston, Texas	1
Green, Mr. R. J. National Aeronautics and Space Administration Washington, D. C.	1
Guenther, Miss Ann Institute for Space Studies National Aeronautics and Space Administration New York, New York	1
Guest, Dr. J. E. University of London Observatory London England	1
Hall, Mr. B. M. Engineering Division Office of the Chief of Engineers Washington, D. C.	1

DISTRIBUTION--Continued

	No. of Copies
Hall, Dr. J. S., Director Lowell Observatory Flagstaff, Arizona	1
Hamilton, Mr. C. E. Marshall Space Flight Center Huntsville, Alabama	1
Hammond, Mr. Harvey, Librarian Hughes Aircraft Company El Segundo, California	1
Harrison, Dr. J. M., Director Geological Survey of Canada Ottawa, Ontario Canada	1
Hearth, Mr. D. P. Planetary Programs Director National Aeronautics and Space Administration Washington, D. C.	1
Hinners, Dr. N. W. Bellcomm, Inc. Washington, D. C.	1
Hodgson, Dr. J. H., Chief Observatories Branch Ottawa, Ontario Canada	1
Howard, Mr. B. T. Bellcomm, Inc. Washington, D. C.	1
Jaffe, Dr. L. D. Jet Propulsion Laboratory California Institute of Technology Pasadena, California	1
James, Mr. D. B. Bellcomm, Inc. Washington, D. C.	1

DISTRIBUTION--Continued

	No. of Copies
Katterfeld, Dr. G. N. Leningrad State University Leningrad USSR	1
Kaula, Mr. William M. Professor of Geophysics I. G. P. P. University of California Los Angeles, California	1
Kopal, Dr. Zdenek Department of Astronomy University of Manchester Manchester, England	1
Kron, Dr. G. E., Director U. S. Naval Observatory Flagstaff, Arizona	1
Kuiper, Professor G. P., Director Lunar and Planetary Laboratory University of Arizona Tucson, Arizona	1
Kummerman, Mrs. N. I., Librarian Geological Survey of Canada Ottawa, Ontario Canada	1
Lafevers, Mr. E. V. Manned Spacecraft Center National Aeronautics and Space Administration Houston, Texas	1
Lamont Geological Observatory Palisades, New York	1
Lincoln Laboratories Massachusetts Institute of Technology Lexington, Massachusetts	1
Low, Dr. G. M., Deputy Administrator National Aeronautics and Space Administration Washington, D. C.	1

DISTRIBUTION--Continued

	No. of Copies
Lowman, Dr. P. D., Jr. Goddard Space Flight Center Greenbelt, Maryland	1
Lundholm, Mr. J. T. National Aeronautics and Space Administration Washington, D. C.	1
Lundquist, Dr. Charles Smithsonian Astrophysical Observatory 60 Garden Street Cambridge, Massachusetts	1
McDonough, Mr. M. P. Manned Spacecraft Center National Aeronautics and Space Administration Houston, Texas	1
Marjaniemi, Mr. Darwin Bendix Aerospace Systems Ann Arbor, Michigan	1
Markow, Mr. Edwin Grumman Aircraft Engineering Corp. Bethpage, New York	1
Martin, Mr. J. S., Jr. Langley Research Center Hampton, Virginia	1
Mayall, Dr. N. U., Director Kitt Peak National Observatory Tucson, Arizona	1
McCord, Dr. Tom Department of Space Sciences Massachusetts Institute of Technology Cambridge, Massachusetts	1
Meine, Dr. -Ing K. -H. Institut für Kartographie und Topographie der Universität Bonn 53 Bonn West Germany	1

	No. of Copies
Meinel, Dr. A. B., Director Steward Observatory University of Arizona Tucson, Arizona	1
Michlovitz, Mr. C. K. National Space Science Data Center Goddard Space Flight Center Greenbelt, Maryland	1
Milwitzky, Mr. Benjamin Office of Manned Space Flight National Aeronautics and Space Administration Washington, D. C.	1
Mitchell, Mr. J. K. Department of Civil Engineering University of California Berkeley, California	1
Molloy, Dr. M. W. National Aeronautics and Space Administration Washington, D. C.	1
Muller, Mr. Paul Jet Propulsion Laboratory Pasadena, California	1
Murray, Professor B. C. Division of Geological Sciences California Institute of Technology Pasadena, California	1
Naugle, Dr. J. E., Associate Administrator Office of Space Science and Application National Aeronautics and Space Administration Washington, D. C.	1
Newell, Dr. H. E., Associate Administrator National Aeronautics and Space Administration Washington, D. C.	1

	No. of Copies
Nicks, Mr. O. W. Deputy Associate Administrator Office of Space Science and Application National Aeronautics and Space Administration Washington, D. C.	1
O'Bryant, Capt. W. T. National Aeronautics and Space Administration Washington, D. C.	1
O'Connor, Dr. J. T. Space Sciences Laboratory University of California Berkeley, California	1
O'Keefe, Dr. J. A., Assistant Chief Laboratory for Theoretical Studies Goddard Space Flight Center Greenbelt, Maryland	1
Orrok, Mr. G. T. Bellcomm, Inc. Washington, D. C.	1
Petrone, Dr. Rocco A. Apollo Program Director National Aeronautics and Space Administration Washington, D. C.	1
Pierce, Dr. K. S. Kitt Peak National Observatory Tucson, Arizona	1
Pickering, Dr. W. H., Director Jet Propulsion Laboratory California Institute of Technology Pasadena, California	1
Rea, Dr. D. G., Deputy Director Planetary Programs National Aeronautics and Space Administration Washington, D. C.	1
Recant, Mr. George Langley Research Center Hampton, Virginia	1

	No. of Copies
Rösch, Dr. Jean, Directeur Observatoire du Pic-du-Midi Pic-du-Midi, France	1
Salisbury, Dr. J. W. Cambridge Air Force Research Laboratories Bedford, Massachusetts	1
Sasser, Mr. James Mapping Sciences Laboratory Manned Spacecraft Center National Aeronautics and Space Administration Houston, Texas	1
Schaefer, Mr. Herbert Marshall Space Flight Center Huntsville, Alabama	1
Scherer, Capt. L. R., Director Apollo Lunar Exploration National Aeronautics and Space Administration Washington, D. C.	1
Schmitt, Dr. H. H. Astronaut Office Manned Spacecraft Center National Aeronautics and Space Administration Houston, Texas	1
Scott, Miss Kathryn Bellcomm, Inc. Washington, D. C.	1
Shoemaker, Dr. E. M. Division of Geological Sciences California Institute of Technology Pasadena, California	1
Shorthill, Mr. R. W. Geo-Astrophysics Laboratory Boeing Scientific Research Laboratories Seattle, Washington	1
Slager, Mr. Charles Defense Intelligence Agency Pentagon Washington, D. C.	1

	No. of Copies
Slight, Mr. J. B. Manned Spacecraft Center National Aeronautics and Space Administration Houston, Texas	1
Smith, Mr. B. A. Department of Astronomy New Mexico State University Las Cruces, New Mexico	1
Smith, Mr. J. W. Research Library Martin-Marietta Corp. Denver, Colorado	1
Soffen, Dr. Gerald A. Viking Project Scientist National Aeronautics and Space Administration Langley Research Center Hampton, Virginia	1
Sonnett, Dr. C. P. Ames Research Center Moffett Field, California	1
South Africa Geological Survey, Director Private Bag 112 Pretoria Union of South Africa	1
Space Sciences Laboratory University of California Berkeley, California	1
Steinbacher, Mr. R. H. Jet Propulsion Laboratory California Institute of Technology Pasadena, California	1
Steinhoff, Dr. E. A. Air Force Missile Development Center Holloman Air Force Base New Mexico	1

	No. of Copies
Stone, Mr. C. A., Director Astro Sciences Center Illinois Institute of Technology Chicago, Illinois	1
Strickland, Col. A. T. Manned Space Science Division National Aeronautics and Space Administration Washington, D. C.	1
Stuhlinger, Dr. Ernst Marshall Space Flight Center Huntsville, Alabama	1
Taback, Mr. Israel Viking Project Office Langley Research Center Hampton, Virginia	1
Thompson, Dr. W. B. Bellcomm, Inc. Washington, D. C.	1
Tiffany, Dr. O. L. Bendix System Division Bendix Corp. Ann Arbor, Michigan	1
Urey, Professor H. C. University of California La Jolla, California	1
Vale, Mr. R. E. Manned Spacecraft Center National Aeronautics and Space Administration Houston, Texas	1
Vaughan, Mr. O. H. Marshall Space Flight Center Huntsville, Alabama	1
von Braun, Dr. Wernher, Director Marshall Space Flight Center Huntsville, Alabama	1
von Tiesenhausen, Mr. G. F. Marshall Space Flight Center Huntsville, Alabama	1

DISTRIBUTION--Continued

	No. of Copies
Weatherred, Mr. C. J. Bendix System Division Bendix Corp. Ann Arbor, Michigan	1
Whipple, Dr. F. L., Director Smithsonian Astrophysical Observatory Cambridge, Massachusetts	1
Wilmarth, Dr. V. L. Manned Spacecraft Center National Aeronautics and Space Administration Houston, Texas	1
Wise, Mr. D. U., Deputy Director Apollo Lunar Exploration Office National Aeronautics and Space Administration Washington, D. C.	1
Young, Mr. A. T. Viking Project Office Langley Research Center Hampton, Virginia	1
Zisk, Dr. S. H. Lincoln Laboratories Massachusetts Institute of Technology Lexington, Massachusetts	1

INTRODUCTION

This annual report is the tenth of a series describing the results of research by the U.S. Geological Survey's Branch of Astrogeologic Studies on behalf of the National Aeronautics and Space Administration under contracts R-66, W-11,775, W-12,872, W-12,388, T-66353G, T-75415, R-09-020-041, and WO-5171. The report was prepared by members of the Branch of Astrogeologic Studies and others who have done work for the branch. This one volume summarizes the results of research carried out between October 1, 1968 and September 30, 1969.

Long-range objectives of the branch program are to investigate and map the geology of the Moon and other planets, to determine the sequence of events that led to the present conditions of the planetary surfaces, and to describe how these events took place. Activities currently leading to these objectives include the following:

(1) Systematic regional mapping of the stratigraphy and structure of the Moon.

(2) Detailed geologic, engineering, and physical studies of selected parts of the lunar surface.

(3) Terrestrial analog studies: including field studies of natural and manmade craters caused by impact, field studies of volcanic features, and field and image analysis studies of terrains dominated by eolian activity.

(4) Laboratory studies of terrestrial rocks and minerals subjected to shock.

(5) Study of the chemical, petrographic, and physical properties of extraterrestrial materials--meteorites, cosmic dust, and returned lunar samples.

(6) Preliminary topographic and geologic evaluation of the Martian surface.

(7) Investigations of techniques and equipment that may lead to the acquisition of data obtainable under a wider variety of planetary environments and suited to more detailed and less equivocal geologic analysis.

(8) Selective ingestigations into some aspects of planetary physics and planetary geodesy where these studies may lead to the acquisition of geologically pertinent information.

(9) Evaluation of planetary exploration strategies as related to the gathering of geologic information.

The above activities are conveniently discussed under five main headings which rather closely parallel the organization of the branch program: Lunar Investigations, Crater Investigations, Cosmic Chemistry and Petrology, Geologic Support for Planetary Missions, and Space Flight Investigations.

Part A, Lunar Investigations.--The first part of the volume describes three programs: (1) lunar geologic mapping, including synoptic compilation of the mapping results at the 1:5,000,000 scale; regional mapping at a scale of 1:1,000,000; Apollo site mapping at the 1:100,000, and 1:25,000, and 1:5,000 scales; a comparison of the geology of 5 early Apollo sites; and Ranger geologic mapping at a variety of scales; (2) lunar physics, including lunar photometry and polarimetry and imaging system design; and (3) lunar engineering geology, including lunar terrain mapping and relative roughness analysis, lunar terrain analysis and trafficability studies, slope stability studies, and estimates of penetration resistance and bearing capacity. Photoclinometry and photogrammetry studies were made in support of terrain trafficability analyses.

Part B, Crater Investigations.--The second part of the volume describes progress in field and laboratory studies of craters and related phenomena. Studies of natural impact structures have been completed at Sierra Madera, Tex., and Flynn Creek, Tenn., and are well advanced at Gosses Bluff, Australia and Decaturville, Mo. Impact-metamorphosed rocks from several large impact structures are being studied in the laboratory, and shock phases of selected minerals are also being studied. Field studies of volcanic craters and related phenomena include Lunar Crater, Nev.; Fernandina caldera in the Galapagos Islands; Diamond Craters,

Bend, Oreg.; Moses Rock and Mule Ear diatremes, Utah; Nunivak, Alaska; Lava Beds National Monument, Calif.; and Mono Craters, Calif. Manmade craters that are being studied include missile-impact craters, impact craters in sand and water, and craters made by chemical explosives.

Part C, Cosmic Chemistry and Petrology.--The third part of the report contains information on the development of microchemical techniques, minor element distribution in igneous rocks, and new laboratory facilities. Recent work on the chemistry and petrology of the Apollo 11 samples, thermal history of tektites, Allende meteorites and the craters, and atmospheric debris from the Revelstoke and Allende fireballs are also discussed.

Part D, Geologic Support for Planetary Missions.--This section contains a very brief summary of the chemistry of the Surveyor landing sites, a summarized version of a strategy for the geologic exploration of the planets, and an assessment of geologic studies (including analog studies) in support of Mars missions. In addition, evaluations of problems in planetary geodesy and physics, of radar studies of Venus, and of theoretical studies of the Venusian atmosphere and the structure of the universe are presented.

Part E, Space Flight Investigations.--The last part includes an abstract of the final report on Surveyor television investigation, an assessment of the Mariner Mars 1971 television experiment, and an evaluation of facsimile camera systems.

The following were published or released in the open files of the U.S. Geological Survey during the period October 1, 1968 to September 30, 1969:

Anderson, A. T., and Greenland, L. P., 1969, Phosphorus fractionation diagram as a quantitative indicator of crystallization differentiation of basaltic liquids: Geochim. et Cosmochim. Acta, v. 33, p. 493-505.

Batson, R. M., 1968, Introduction, in Catalog of Surveyor television pictures: Natl. Space Sci. Data Center, Natl. Aeronautics and Space Adm., NSSDC 68-10, p. 1-3.

_____1969, Photogrammetry with surface-based images: Appl. Optics, v. 8, no. 7, p. 1315-1322.

Bingham, J. W., and Grolier, M. J., 1969, Geology and groundwater conditions in parts of Grant, Adams, and Franklin Counties, Washington: U.S. Geol. Survey open-file report, 85 p.

Borgeson, W. T., and Batson, R. M., 1969, Photogrammetric calibration of Apollo film cameras: U.S. Geol. Survey open-file report, 14 p.

Brett, P. R., 1968, Opaque minerals in drill cuttings from Meteor Crater, Arizona, in Geological Survey Research 1968: U.S. Geol. Survey Prof. Paper 600-D, p. 179-180.

Cannon, P. J., 1968, Pleistocene stream piracy in southwestern Oklahoma: Oklahoma Geol. Notes, v. 28, no. 6, p. 183-187.

Chao, E. C. T., 1968, Pressure and temperature histories of impact metamorphosed rocks--based on petrographic observations, in French, B. M., and Short, N. M., eds., Shock metamorphism of natural materials: Baltimore, Mono Book Corp., p. 135-158.

Chao, E. C. T., and Bell, P. M., 1969, Annealing characteristics of dense feldspar glass: Carnegie Inst., Washington, Year Book 67, p. 126-130.

Cummings, David, 1968, Geologic map of the Zuni Salt Lake volcanic crater, Catron County, New Mexico: U.S. Geol. Survey Misc. Geol. Inv. Map I-544.

Cummings, David, 1968, Shock deformation of biotite around a nuclear explosion, in French, B. M., and Short, N. M., eds., Shock metamorphism of natural materials: Baltimore, Mono Book Corp., p. 211-217.

_____1969, Geologic map of Lunar Orbiter site III-P-11, Oceanus Procellarum south of the equator [scale 1:100,000]: U.S. Geol. Survey open-file report.

_____1969, Preliminary geologic map of the Clavius quadrangle of the Moon [scale 1:1,000,000]: U.S. Geol. Survey open-file report.

Duke, M. B., 1969, Surveyor alpha-scattering data [tech. comment]: Science, v. 165, no. 3892, p. 515.

_____1968, Shergotty meteorite: magmatic and shock metamorphic features, in French, B. M., and Short, N. M., eds., Shock metamorphism of natural materials: Baltimore, Mono Book Corp., p. 613-621.

_____1969, Laboratory for returned lunar material: Contamination Control, v. 8, no. 10, p. 28.

Eggleton, R. E., 1968, (Geologic evaluation of) Site V-34, Fra Mauro, in Lunar Orbiter photo-data screening group, A preliminary geologic evaluation of areas photographed by Lunar Orbiter V including an Apollo landing analysis of one of the areas: Natl. Aeronautics and Space Adm., Langley Research Center, Langley Working Paper 506, p. 87-89.

_____1968, (Geologic evaluation of) site V-45.1, Gruithuisen domes, in Lunar Orbiter photo-data screening group, A preliminary geologic evaluation of areas photographed by Lunar Orbiter V including an Apollo landing analysis of one of the areas: Natl. Aeronautics and Space Adm., Langley Research Center, Langley Working Paper 506, p. 90-92.

Freeberg, J. H., 1969, Terrestrial impact structures--A bibliography 1965-68: U.S. Geol. Survey Bull. 1320, 39 p.

_____1969, Bibliography of the lunar surface: U.S. Geol. Survey open-file report, 697 p.

Gambell, Neil, and Lucchitta, B. K., 1968, A limitation of first generation Lunar Orbiter negatives as applied to photoclinometry: U.S. Geol. Survey open-file report, 11 p.

Gottfried, David, Greenland, L. P., and Campbell, E. Y., 1968, Variation of Nb-ta, Zr-Hf, Th-U, and K-Cs in two diabase-granophyre suites: Geochim. et Cosmochim. Acta, v. 32, p. 925-947.

Greenland, L. P., and McLane, John, 1969, Determination of germaniun in silicates by neutron activation analysis; in Geological Survey Research 1968: U.S. Geol. Survey Prof. Paper 650-C, p. C152-C154.

Harbour, Jerry, 1969, Geologic mapping of the Moon: Allemeine Vermessungs-Nachrichten, H. 5/1969, p. 211-219.

_____1969, Geologic mapping of the Moon: Geotimes, v. 14, no. 7, p. 14-18.

Howard, K. A., 1968, Flow direction in triclinic folded rocks: Am. Jour. Sci., v. 266, no. 9, p. 758-765.

_____1969, Lava channels in northeastern California [abs.]: Am. Geophys. Union Trans., v. 50, no. 4, p. 341.

Howard, K. A., and Simkin, Tom, 1969, 1968 collapse of Fernandina caldera, Galapagos Islands [abs.]: Am. Geophys. Union Trans., v. 50, no. 3, p. 344.

Jackson, E. D., and Wilshire, H. G., 1968, Chemical composition of the lunar surface at the Surveyor landing sites: Jour. Geophys. Research, v. 73, no. 24, p. 7621-7630.

James, O. B., 1969, Jadeite: shock-induced formation from oligoclase, Ries Crater, Germany: Science, v. 165, no. 3897, p. 1005-1008.

Jones, R. S., 1968, Gold in meteorites and in the Earth's crust: U.S. Geol. Survey Circular no. 603.

_____1969, Gold in igneous, sedimentary, and metamorphic rocks: U.S. Geol. Survey Circular no. 610.

_____1969, Gold in minerals and the composition of native gold: U.S. Geol. Survey Circular no. 612.

Jones, R. S., 1969, Gold in water, plants, and animals: U.S. Geol. Survey Circular no. 625.

Lunar Sample Preliminary Examination Team (including E. C. T. Chao, M. J. Grolier, and E. M. Shoemaker), 1969, Preliminary examination of lunar samples from Apollo 11: Science, v. 165, no. 3899, p. 1211-1227.

Masursky, Harold, 1969, Lunar exploration targets: Astronautics and Aeronautics, v. 7, no. 1, p. 42-49.

Masursky, Harold and McCauley, J. F., 1968, An investigation of the regional geology of Mars as part of the Mariner 1971 Television Experiment, 24 p.

May, Irving and Cuttitta, Frank, 1968, New instruments in geochemistry, in New instrumental techniques in geochemical analysis: New York, Plenum Pub. Co., p. 112-142.

McCauley, J. F., 1968, Preliminary photogeologic map of the Orientale basin, figure 6 in Ulrich, G. E., Advance systems traverse research project report: U.S. Geol. Survey open-file report, p. 32-33.

_____1969, Moon probes: Morristown, New Jersey, Silver Burdett Co., 64 p.

dence for lunar differentiation? [abs.]: Am. Geophys. Union Trans., v. 50, no. 4, p. 229.

_____1969, Geologic map of the Alphonsus GA region of the Moon: U.S. Geol. Survey Misc. Geol. Inv. Map I-586.

McGetchin, T. R., 1969, Source and emplacement of kimberlite at Moses Rock dike, Utah [abs.]: Am. Geophys. Union Trans., v. 50, no. 4, p. 345.

_____1969, A crustal-upper mantle model based on crystalline rock fragments in a kimberlite dike [abs.]: Am. Geophys. Union Trans., v. 50, no. 4, p. 345.

_____1969, On the thermal history of tektites [abs.]: 3rd Internat. Tektite Symposium, Corning, New York, April, 1969.

McGetchin, T. R., 1969, Titanoclinohumite and other hydrous minerals in the Earth's interior and the problem of lunar water [abs.]: Am. Astronautical Soc. Mtg., Denver, Colorado, June, 1969.

McGetchin, T. R., and Silver, L. T., 1969, A crustal-upper mantle model for the Colorado Plateau based on observations of crystalline rock fragments in a kimberlite dike [abs.], in Phase Transitions, Earth's Interior Internat. Symposium: Australian Acad. Sci., Canberra, 1969.

Milton, D. J., 1968, Structure of the Henbury meteorite craters, Australia, in French, B. M., and Short N. M., eds., Shock metamorphism of natural materials: Baltimore, Mono Book Corp, p. 115-116.

_____1968, Reconnaissance geologic map of part of the Milan quadrangle, New Hampshire-Maine and the Percy quadrangle, New Hampshire.

_____1969, Gosses Bluff astrobleme, Australia--shatter cones [abs.]: Am. Geophys. Union Trans., v. 50, no. 4, p. 220.

_____1969, Astrogeology in the nineteenth century: Geotimes, v. 14, no. 6, p. 22.

_____1969, Impact metamorphism at Gosses Bluff and Mataranka, N. T., Australia [abs.]: 3d Internat. Tektite Symposium, Corning, New York, April 1969.

Moore, H. J., 1969, Subsurface deformation resulting from missile impacts: U.S. Geol. Survey Prof. Paper 650-B, p. B107-B112.

_____1969, Ejecta from lunar craters [abs.]: Am. Geophys. Union Trans., v. 50, no. 4, p. 221.

Moore, H. J., Pike, R. J., and Ulrich, G. E., 1969, Lunar terrain and traverse data for Lunar Roving Vehicle design study: U.S. Geol. Survey internal report for NASA, Marshall Space Flight Center, 246 p.

Morris, E. C., Batson, R. M., Holt, H. E., Rennilson, J. J., Shoemaker, E. M., and Whitaker, E. A., 1968, Television observations from Surveyor VI, Surveyor VI mission report, Part II: Science results: Jet Propulsion Lab. Tech. Rept. 32-1262, p. 9-45.

Naeser, C. W., 1969, Fission-track dating of accessory minerals in igneous and metamorphic rocks [abs.]: Nuclear Track Registration in Insulating Solids and Applications Internat. Topical Conf: Clermont-Ferrand, France, May 1969, p. 46.

_____1969, Etching fission tracks in zircon: Science, v. 165, p. 388.

Naeser, C. W., and Dodge, F. C. W., 1969, Fission-track ages of accessory minerals from rocks of the Sierra Nevada batholith: Geol. Soc. America Bull., v. 80, no. 11, p. 2201-2212.

Naeser, C. W., Dodge, F. C. W., and Kistler, R. W., 1968, Fission-track ages of accessory minerals from rocks of the Sierra Nevada batholith [abs.]: Geol. Soc. America Ann. Mtg., 1968, p. 214.

Naeser, C. W., and Faul, Henry, 1969, Fission-track annealing in apatite and sphene: Jour. Geophys. Research, v. 74, p. 705.

Page, N. J, Calk, L. C., and Carr, M. H., 1968, Problems of small-particle analysis with the electron microprobe, in Geological Survey Research 1968: U.S. Geol. Survey Prof. Paper 600-C, p. C31-C37.

Pike, R. J., 1969, Meteoritic origin and consequent endogenic modification of large lunar craters: A study in analytical geomorphology: U.S. Geol. Survey open-file report, 404 p.

Pohn, H. A., and Offield, T. W., 1969, Lunar crater morphology and relative age determination of lunar geologic units: U.S. Geol. Survey open-file report, 35 p.

Pohn, H. A., Radin, H. W., and Wildey, R. L., 1969, The Moon's photometric function near zero phase-angle from Apollo 8 photography: Astrophys. Jour., v. 157, p. L193-L196.

Roddy D. J., 1969, Geological Survey activities, in Dudash, J. J., ed., Operation Prairie Flat Preliminary Report: Defense Atomic Support Agency, Defense Dept., DASA 228-1, p. 317-333.

_____1969, Preliminary report on the surface geology and ground deformation at the AN/FO craters: Defense Atomic Support Agency, Defense Dept., 15 p.

Roddy, D. J., and Davis, L. K., 1969, Shatter cones at TNT explosion craters [abs.]: Am. Geophys. Union Trans., v. 50, no. 4, p. 220.

Roddy, D. J., Jones, G. H. S., and Diehl, C. H. H., 1969, Similarities of 100 and 500 ton TNT explosion craters and proposed comet impact craters [abs.]: Am. Geophys. Union Trans., v. 50, no. 4, p. 220.

Rozema, W. J., 1968, The use of spectral analysis in describing lunar surface roughness: U.S. Geol. Survey open-file report, 34 p.

Schumm, S. A., 1969, Experimental studies on the formation of lunar surface features by gas emission--a preliminary report: U.S. Geol. Survey open-file report, 22 p.

Schumm, S. A., and Simons, D. B., 1969, Lunar rivers or coalesced chain craters?: Science, v. 165, no. 3889, p. 201.

Scott, D. H., 1969, Geology of the southern Pancake Range and Lunar Crater volcanic field [abs.]: Ann Arbor, Mich., Dissertation Abs.

Shoemaker, E. M. (Principal Investigator), Morris, E. C., Batson, R. M., Holt, H. E., Larson, K. B., Montgomery, D. R., Rennilson, J. J., and Whitaker, E. A., 1968, Television observations from Surveyor, in Surveyor project final report, Part II, Science results: Jet Propulsion Lab. Tech. Rept. 32-1265, p. 21-136.

Shoemaker, E. M. (Principal Investigator), Morris, E. C., Batson, R. M., Holt, H. E., Larson, K. B., Montgomery, D. R., Rennilson, J. J., and Whitaker, E. A., 1969, Television observations from Surveyor, in Surveyor program results: Natl. Aeronautics and Space Adm. Spec. Rept. SP 184, p. 19-128.

Simkin, Tom, and Howard, K. A., 1968a, Caldera collapse in the Galapagos Islands, 1968 [abs.]: Geol. Soc. America, Program 1968 Ann. Mtg., p. 280.

_____1968b, 1968 Collapse of Fernandina caldera, Galapagos Islands: Smithsonian Institution Center for Short-Lived Phenomena, Event Rept., 16 December, 1968, 22 p.

Smith, E. I., 1969, Rümker Hills: A volcanic plateau in the Oceanus Procellarum, Moon [abs.]: Am. Geophys. Union Trans., v. 50, no. 4, p. 229.

Stuart-Alexander, D. E., 1968, Preliminary geologic map of site V-8, in A preliminary geologic evaluation of areas photographed by Lunar Orbiter V: Natl. Aeronautics and Space Adm., Langley Research Center, Langley Working Paper 506, p. 29.

_____1968, Low-temperature formation of wollastonite: Geol. Soc. America, Spec. Paper 115, p. 216-217.

Thompson, J. B., Jr., Robinson, P., Clifford, T. N., and Trask, N. J., 1968, Nappes and gneiss domes in west-central New England, in Studies in Appalachian geology: Northern and maritime: New York, John Wiley and Sons--Interscience Pub., p. 203-218.

Tilling, R. E., Greenland, L. P., and Gottfried, David, 1969, Distribution of scandium between coexisting biotite and hornblende in igneous rocks: Geol. Soc. America Bull., v. 80, p. 651-668.

Titley, S. R., and Trask, N. J., 1968, Geologic map of the ellipse West One area [scale 1:25,000]: U.S. Geol. Survey open-file report.

Trask, N. J., 1968, Geologic map of the ellipse Central One area [scale 1:25,000]: U.S. Geol. Survey open-file report.

_____1968, Geologic mapping of potential early Apollo landing sites [abs.]: Geol. Soc. America, Cordilleran Sec., 64th Ann. Mtg, Tucson, Arizona, Program, p. 125.

_____1969, Geologic map of the Sabine DM region of the Moon [scale 1:50,000]: U.S. Geol. Survey Misc. Geol. Inv. Map I-594.

_____1969, Geology of early Apollo landing sites of set C: U.S. Geol. Survey open-file report, 27 p.

Trask, N. J., and Holt, H. E., 1969, Moon, television-camera pictures, pt. of 3 pt. art., in McGraw Hill Yearbook of Science and Technology: New York, McGraw Hill Book Co., p. 218-222.

Van Allen, J. A., and others (including R. L. Wildey), 1969, The outer solar system: a program for exploration: Nat. Acad. Sci., Space Sci. Board, p. 1-85.

Wildey, R. L., 1967, Spatial filtering of astronomical photographs: Astron. Soc. Pacific Pub., v. 79, p. 220-225.

_____1967, On the treatment of radiative transfer in the lunar diurnal heatflow: Jour. Geophys. Research, v. 72, p. 4765-4767.

_____1967, Spatial filtering of astronomical photographs: II theory: Astron. Jour., v. 72, p. 884-886.

_____1969, Die laser in die astronomie: Laser: und angew. Strahlentechnik, v. 2, p. 27-37.

Wilhelms, D. E., 1969, Photogeologic mapping of the Moon, in Merifield, P. M., ed., Interpretation of extraterrestrial imagery: Photogramm. Eng., v. 35, no. 5, p. 480-482.

_____1969, Geologic interpretation of Lunar Orbiter photographs, in Merifield, P. M., ed., Interpretation of extraterrestrial imagery: Photogramm. Eng., v. 35, no. 5, p. 486-490.

Wilhelms, D. E., and McCauley, J. F., 1969, Volcanic materials in the lunar terrae--Orbiter observations: Am. Geophys. Union Trans., v. 50, no. 4, p. 230.

_____1969, Preliminary geologic map of the near side of the Moon [scale 1:5,000,000]: U.S. Geol. Survey open-file report.

Wilhelms, D. E., Stuart-Alexander, D. E., and Howard, K. A., 1969, Preliminary interpretations of lunar geology, in Lunar and space report: Natl. Aeronautics and Space Adm., v. 1, p. 2, 18-28.

Wilshire, H. G., 1968, Preliminary geologic map of Lunar Orbiter site II-P-11 [scale 1:100,000]: U.S. Geol. Survey open-file report.

PART A. LUNAR INVESTIGATIONS

Lunar Mapping

During contract year 1969 and in the part of contract year 1970 preceding this writing, milestones were reached in all four of the systematic lunar mapping programs. A map of the near side at a scale of 1:5,000,000 was prepared and distributed. Mapping of the 44 1:1,000,000-scale quadrangles was completed in preliminary form and publication or final preparation for publication brought to the half way point. Nineteen revised early-Apollo site maps (of 7 sites out of the 8 mapped in preliminary form) have been transmitted to the Manned Spacecraft Center, and the 13 definitely intended for publication either have been submitted for publication or are nearly ready to be. Two of the Ranger series of 6 maps have been published, one is at the printers, and the others are nearly ready to be submitted for publication.

Compilation at a scale of 1:5,000,000 (Contract R-66).--A regional compilation entitled "Preliminary geologic map of the near side of the Moon" was completed by Don E. Wilhelms and John F. McCauley and released in the open files. The map's coverage was extended from that reported last year (the equatorial belt, 32°N.-32°S.) to include the entire area covered by the 44 ACIC 1:1,000,000-scale LAC's. The base is the ACIC orthographic LEM-1 photographic mosaic at a scale of 1:5,000,000. Four major categories of units were mapped: Circumbasin materials, crater materials, terra materials, and mare and other dark materials. These are divided into 44 units and type areas are given for each unit. The map is available either in the form of color photographic prints at reduced scales or as black and white ozalid prints at 1:5,000,000. An explanatory text and expanded unit explanation were completed but have not yet been open-filed. The map will be published as soon as it is reviewed.

A simplified map derived from this geologic map has also been prepared. This map, not yet open-filed, shows 11 provinces interpreted as being characterized by different types or ages of

internal activity. These range from the southern highland province of large craters, which is believed to have been little altered by internal activity since its formation early in lunar history, to provinces in both the terrae and maria that are believed to have been active in relatively recent lunar history.

Mapping at a scale of 1:1,000,000 (Contract R-66).--The following five 1:1,000,000-scale quadrangles have been completed by their authors and are being prepared for distribution in ozalid form: Tycho, by H. A. Pohn; Schickard, by T.N.V. Karlstrom; Geminus, by M. J. Grolier; Wilhelm, by R. S. Saunders; and Aristoteles, reassigned to B. K. Lucchitta. This completes preliminary mapping of all 44 1:1,000,000-scale LAC quadrangles (fig. 1).

The following maps are nearly ready for distribution as I-maps: Sinus Iridum, by G. G. Schaber, and J. Herschel, by G. E. Ulrich.

The following four maps have been completed by their authors and reviewed, and either have been submitted for publication or are ready for final check by the Technical Reports Unit prior to submission for publication: Cassini, by N. J. Page; Schiller, by T. W. Offield; Rupes Altai, by L. C. Rowan; and Colombo, by D. P. Elston. The last two are in the equatorial belt of 28 quadrangles where the mapping program began; Cassini adds to the coverage of the northern part of the Imbrium basin; and Schiller will be the first of the far southern-highland maps to be submitted for publication. With the publication of these maps and of Sinus Iridum and J. Herschel, the conversion of the preliminary to published maps will be half complete--22 out of 44.

Progress was made in contract year 1969 on the majority of the other 22 quadrangles, but estimated dates of completion cannot now be given due to the uncertainties of the work load on new Apollo site maps in the current contract year. Reassignments of 1:1,000,000 quadrangles since last year's report are: Macrobius to H. A. Pohn and C. J. Casella, Cleomedes to C. J. Casella and A. B. Binder,

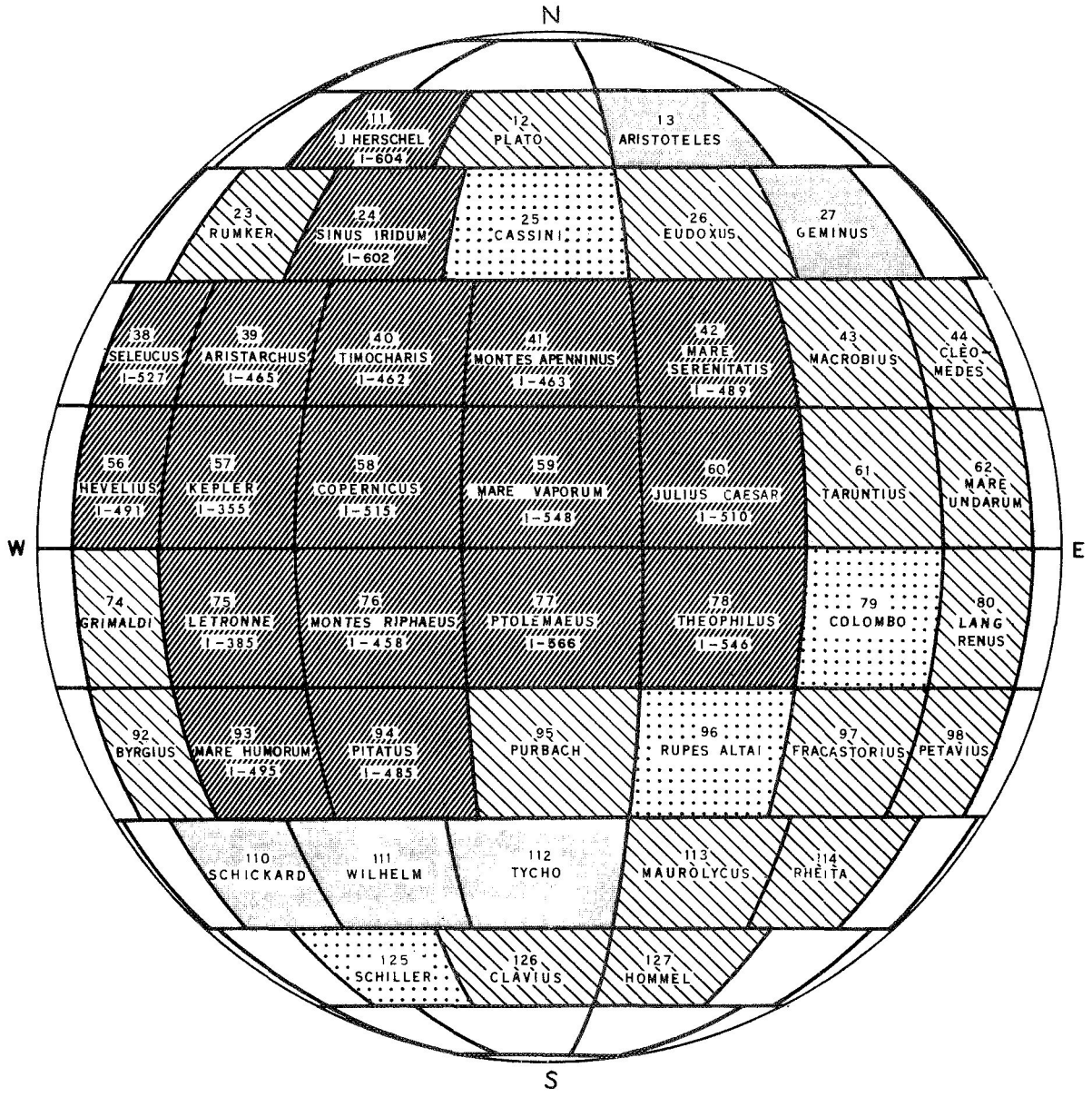

Figure 1. Index map of Moon showing status of mapping at the 1:1,000,000 scale as of September 1969.

Eudoxus to F. El-Baz, and Fracastorius to D. E. Stuart-Alexander and R. W. Tabor.

Apollo site mapping (Contract T-66353G).--Geologic maps of the 5 early Apollo landing sites of set C at scales of 1:100,000 and 1:25,000 were revised, standardized, and transmitted to the Manned Spacecraft Center during contract year 1969. A map of a sixth site in the Flamsteed ring (III P-12) was also completed at a scale of 1:100,000 only. Maps of a seventh site (III P-9) at scales of 1:100,000 and 1:25,000 were transmitted to the Manned Spacecraft Center early in contract year 1970. An estimated publication schedule for all early Apollo site maps is included as Table 1. Maps at a scale of 1:5,000 designed for use by astronauts and ground personnel during Apollo missions were made for sites #1 through #5 and #7; these maps will not be published. A geologic comparison and evaluation of the 5 Apollo sites of set C was completed by Trask (1969); an abstract of that paper follows:

> A geologic comparison of the 5 potential early Apollo landing sites of set C reveals significant similarities and differences among them. No two of the sites are identical and a consideration of the geology of each site will be essential to complete interpretation of returned lunar samples and observations. Geologic maps of each site have been prepared at scales of 1:5,000, 1:25,000, and 1:100,000.
>
> Features emphasized on the 1:5,000 scale maps are common to all the sites and include mainly the widespread lunar regolith and small craters with a variety of ages and origins. Because they cover the lunar surface and because mobility will be limited on early missions, these ubiquitous features will be the main objects of scientific inquiry during the first manned landings.
>
> Regional geologic differences among the sites are more clearly shown on the 1:25,000-and 1:100,000-scale maps. Mare materials in sites 2 and 3 belong mainly to the Imbrian System; the materials in site 3 appear to be younger than those in site 2. Mare materials in sites 4 and 5 belong entirely to the Eratosthenian System. Materials in site 1 belong mostly to a young mantle of relatively low-cohesion material, assigned to the Copernican System, covering an older cratered terrain, that is probably part of the terrae; typical mare material occurs only in the eastern extremity of the site. Ray

materials and secondary impact craters related to large rayed primary impact craters are present in several of the sites.

Table 1.--Publication status of geologic maps of early Apollo landing sites. 1/

Abbreviated map title	Scale	Author	Director's Approval	Estimated Publication Date
Maskelyn DA Region II P-2 (I-616)	1:100,000	Carr	6/69	3/70
Apollo site 1 (I-617)	1:25,000	Wilhelms	6/69	4/70
Sabine D Region II P-6 (I-618)	1:100,000	Grolier	6/69	1/70
Apollo site 2 (I-619)	1:25,000	Grolier	6/69	12/69
Oppolzer A Region	1:100,000	Rowan	7/69	4/70
Apollo site 3 (I-621)	1:25,000	Trask	7/69	5/70
Wichmann CA Region III P-11	1:100,000	Cummings		
Apollo site 4 and 4R	1:25,000	West & Cannon	11/69	7/70
Maestlin G Region	1:100,000	Carr & Titley	8/69	11/69
Apollo site 5 (I-623)	1:25,000	Titley & Trask	8/69	11/69
Flamsteed K Region III P-12	1:100,000	Offield		
Apollo site 6R	1:25,000	West		
Lansberg P Region III P-9	1:100,000	Pohn		
Apollo site 7	1:25,000	Cannon		

1/ U. S. Geological Survey publication numbers in parentheses.

Geologic maps in support of advanced Apollo missions were started for the following sites: Fra Mauro, Rima Bode, Censorinus, Tycho, Descartes, Marius Hills, Apennine/Hadley, and Copernicus central peak.

Ranger geologic mapping (Contract WO-5171).--The status of Ranger geologic mapping is shown in Table 2. Trask (in press) summarized some of the results of the Ranger geologic mapping for a symposium on planetary atmospheres and surfaces. An abstract of that paper follows:

> Photographs from the Ranger probes provided the first direct evidence on the fine-scale topography of the Moon and showed that the surface is relatively smooth over slope distances of 1 meter. In addition to craters, elements contributing to the topography at this scale are the closely spaced ridges and troughs of lunar patterned ground. Blocks in the size range 0.5 to several meters were not seen in the Ranger pictures, perhaps because of the limited sampling at three widely separated points. Ranger VII photographs showed the preponderance of shallow elongate to circular craters along rays. Ranger VIII photographs were notable in portraying with new clarity the craters Sabine and Ritter, which appear to be of internal rather than impact origin. Ranger IX photographs of the floor of the crater Alphonsus contained data from which a complicated geological history of the floor can be deciphered.

Table 2.--Status of Ranger geologic maps.

Map [1/]	Scale	Author	Publication Date
RLC 3	1:100,000	Moore & Eggleton	12/70 est.
RLC 4	1:10,000	Titley	12/70 est.
RLC 9 (I-594)	1:50,000	Trask	6/69
RLC 11	1:5,000	Cannon & Rowan	12/70 est.
RLC 14	1:250,000	Carr	1/70 est.
RLC 15	1:50,000	McCauley	6/69

1/ Publication numbers in the U. S. Geological Survey I-map series shown in parentheses.

Lunar Physics

Investigations of lunar physics comprise two categories: (1) lunar and planetary photometry (Contract R-09-020-041), and (2) lunar and planetary polarimetry (Contract R-66). R. L. Wildey studied the problem of the observational definition of the variability in form of the lunar photometric function over the lunar surface. The problem was approached from the point of view of two orbiting Apollo experiments at the extremes of complexity and simplicity. An electromechanically rastered photoelectric-photometric-camera was designed to select the geometry of illumination and observation by scanning a series of lines from horizon to horizon in the spacecraft orbital plane at approximately rapid frame rate, matching published Apollo constraints and employing the 500 Kc-wide video channel. This approach would, at least in quantified fashion and through a series of missions, delineate the photometric function in its general form as a function of selenographic coordinates as well as lighting and viewing geometry. An alternate approach using very simple hardware and low bit rate invokes complementary Earth-based observations. The device is a simple nader-pointing photometer. The λ, β track is regained and observed from Earth by astronomical photoelectric photometry. From the spacecraft a broad variation in phase angle is seen, however, always at zero luminance longitude. The same points observed from Earth allow a variety of phase angle and luminance longitudes, however, with the usual forced correlation through λ and β and the limited libration. By also observing correspondence points using waxing-waning and north-south symmetry and the reciprocity principle, and by using the map of the normal albedo of the Moon by Pohn and Wildey a five-fold degeneracy in the definition of lighting-viewing geometry over the lunar surface can be achieved for such an investigation. A quantitative evaluation of the error attendant on the assumption that the Moon has one and only one photometric function is thus afforded on a basis superior to any heretofore possible.

R. L. Wildey and H. A. Pohn, with the collaboration of H. W. Radin of Bellcomm, Inc., made measurements of the lunar photometric function near zero phase angle. Such investigations are possible without complete photographic coverage. A relative D-log E curve at appropriate color-temperature and a knowledge of the focal length of the camera proved sufficient. These investigations are impossible from Earth due to lunar eclipse.

A suitable Heiligenschein frame was found among the Apollo 8 photographs. It was found that the upsurge in brightness from a phase angle of 1.5° to zero, which is just the range unobservable from Earth, was 19 percent. Wildey and Pohn had previously extrapolated logarithmically their Earth-based photometry and obtained a value of only 5 percent. In later measurements of the normal albedo of the Apollo 11 landing sight, which was fortuitously in Heiligenschein on an Apollo 10 frame, this same upsurge was only 7.2 percent. These results represent the first clear detection of the non-uniqueness of the lunar photometric function over the lunar surface. Furthermore, Tranquility Base is in a mare area, whereas the other Heiligenschein was measured on plains in the highlands. A suspected lithologic correlation should be investigated.

Lunar Engineering Geology

Lunar terrain mapping and relative roughness analysis (Contract W-11,775).--A final report on lunar terrain mapping and relative roughness analysis was completed by L. C. Rowan, J. F. McCauley, and Esther A. Holm and is now in press as a U. S. Geological Survey Professional Paper. The abstract follows.

> Terrain maps of the equatorial zone (long 70°E. to 70°W. and lat 10°N. to 10°S.) were prepared at scales of 1:2,000,000 and 1:1,000,000 in order to classify lunar terrain with respect to roughness and to provide a basis for selecting sites for Surveyor and Apollo landings as well as Ranger and Lunar Orbiter photographs. The techniques developed as a result of this effort can be applied to future planetary exploration.
>
> At the 1:1,000,000 scale, using the best available Earth-based observational data and photographs, U. S. Geological Survey lunar geologic maps, and U. S. Air Force Aeronautical

Chart and Information Center LAC charts, lunar terrain is described by qualitative and quantitative methods and divided into four fundamental classes: maria, terrae, craters, and linear features. Some 35 subdivisions are defined and mapped throughout the equatorial zone, and, in addition, most of the map units are illustrated.

The terrain types were analyzed quantitatively to characterize and order their relative roughness characteristics. Approximately 150,000 east-west slope measurements made by a photometric technique (photoclinometry) in 51 sample areas indicate that algebraic slope frequency distribution are Gaussian, so that arithmetic means and standard deviations accurately describe the distribution functions. The algebraic slope component frequency distributions were particularly useful for rapidly determining relative roughness of terrain.

The statistical parameters that best describe relative roughness are the absolute arithmetic mean, the algebraic standard deviation, and the percentage of slope reversal. Statistically derived relative relief parameters are desirable supplementary measures of relative roughness in the terrae. Extrapolation of relative roughness for mare is demonstrated using Ranger VII slope component data and regional maria slope data, as well as the data reported here. It appears that, for some morphologically homogeneous mare areas, relative roughness can be extrapolated for the large scales from measurements at small scales.

Lunar Terrain Analysis (Contract T-66353G) and Trafficability (Contract W-12,388).--During contract year 1969, R. J. Pike examined the surface geometry of over 200 lunar and terrestrial terrains at varying levels of generalization and using data from several different sources. Quantitative results in the form of base length slope and slope curvature statistics and frequency distributions (Moore, Pike, Ulrich, 1969), power spectral density (PSD) functions (Rozema, 1968), slope reversal frequencies, elevation statistics, and information on terrain slopes between slope reversals were generated in support of the Apollo program, the lunar roving vehicle program, and the continuing U. S. Geological Survey program of planetary surface form classification.

The initial version of a flexible and comprehensive terrain analysis computer program is now operational and is being used to generate all of the above-mentioned measures for both lunar and terrestrial topographic data in profile. The entire program can be altered to handle matrix data in the future.

Over 80 lunar terrain samples have been processed on the IDT equipment and with the Langley II photoclinometric program, using imagery from Lunar Orbiter missions II, III, IV, and V, and include resolutions between 1m and 35 m. All statistical results from lunar photoclinometry are being catalogued together with PSD curves and photographs as a convenience for future reference and mission planning. Lunar photometric samples show a wide variance in terrain type and relative roughness at all levels of generalization, although the best constrasts seem to be evident at a 10-15 m resolution rather than at a 1-5 m resolution. Significant limitations of photometric lunar terrain data as derived from existing IDT facilities and computer software are evident, most notably in rougher areas, such as block fields surrounding fresh craters and steeply sloping terrains in deep shadow or bright sun.

The advent of Apollo command module photography (notably Apollo 8 and 10) has provided photogrammetric terrain data to supplement and eventually supplant photogrammetric reduction of Lunar Orbiter imagery. Apollo topographic data, at a resolution of 35-100 m, complement and provide a check on photoclinometric measurements. A preliminary comparison of the two techniques suggests strongly that photogrammetry portrays lunar terrain as being somewhat rougher than it is while photometric reduction smooths out the topography. Clearly, both types of data are necessary for valid appraisals of lunar surface roughness conditions and regional variations of terrain geometry.

Complementary quantitative investigations of terrestrial topography have been undertaken along two principal approaches. Over two dozen detailed profiles have been surveyed on probable analogs of lunar terrains using elevations obtained at one meter

intervals or taken from large-scale contour maps. These terrains have included nine samples of topography in the San Francisco volcanic field near Merriam Crater, Arizona, and four samples of the rim of the nuclear experimental crater Danny Boy. The Merriam Crater samples appear to be analogous to some lunar terrain types sampled photometrically in the Marius Hills region of the Moon. In particular, the PSD curve describing a Quaternary basalt spatter cone in the Merriam area closely resembles the curve derived for a Marius Hills feature classified as a pierced or breached volcanic cone.

The second part of the terrestrial terrain data study has used 21 x 21 matrices of elevations read from selected U. S. Geological Survey 1:24,000 topographic quadrangles at a constant increment of 200 feet (61 meters). The 80 samples for which descriptive statistics have been generated include a variety of terrain geometry representative of most topography in the United States, with emphasis on volcanic and eolian surfaces. The range of average slope values coincides more closely with results of lunar photogrammetry than it does with data derived from photoclinometry. A tentative relationship between average slope and maximum slope has been obtained from these data. Additionally, the hypsometric integral, a measure used to describe terrestrial fluvial watersheds, has been shown from these data to be identical to the elevation:relief ratio, a much more easily derived parameter, thus affording a far less time-consuming method for drainage basin analysis.

All data on base length slope angle have been used in a continuing study of the effects of topographic scale on slope. The logarithm of average slope decreases with increasing logarithm of base length systematically at a power of about 0.25. Although the relationship may flatten out for slope lengths under 10 m, the mean slope:base length curves can be used to predict mean slope values of lunar terrains at resolutions far below those for which data are available in many areas. In turn, mean slope values can be used to predict entire slope-frequency distributions, using

a technique developed from previous work in terrestrial terrain analysis by Walter F. Wood.

All-in-all, a significant proportion of the lunar surface has been shown or inferred to be impassable to wheeled vehicles of the type contemplated for use in future lunar surface missions. Specifically, fresh craters of all size ranges, the rims of younger mare basins, the rim's large craters regardless of age, and apparent fresh volcanic terrains will be difficult or impossible to traverse. Terrestrial analogs of lunar topography can be selected, on the basis of quantitative criteria, for the evaluation of lunar roving vehicle performance.

Bearing capacity studies (Contract R-66).--Estimates by H. J. Moore of static bearing capacities based on boulder track data from Lunar Orbiter II and III photographs yield values corresponding to lunar soils with cohesions of 10^3 dynes/cm^2 failing by general shear and with friction angles between 10° and 30° (averaging 17°).

Considerable effort has been made assisting Dr. James Mitchell and John Hovland of the University of California (Berkeley) in their study of lunar boulder tracks. Such assistance includes: (1) giving technical advice on photographs, (2) furnishing them 35X enlargements of Lunar Orbiter photographs, and (3) furnishing them selected profiles along lunar boulder tracks made with photogrammetric data. Their studies of boulder tracks on Lunar Orbiter V photographs (mainly) yield higher friction angles than those determined by Moore.

A paper entitled "Bearing capacity of lunar surface materials" was completed by G. L. Martin, and is now in the final stages of review before publication. Following is the abstract of that paper:

> A proposed method of indirectly evaluating the bearing capacity of near-surface lunar materials is investigated with respect to the influence of seismic activity. Specifically, failed lunar slopes are analyzed in order to determine probable strength parameters of lunar soils. Methods of slope stability analysis that could be used in the indirect evaluation are reviewed and stability charts,

based on the "method of slices," are developed with the inclusion of horizontal seismic acceleration as one of the variables. Finally, extreme values of lunar bearing capacity, based on data from Lunar Orbiter II photographs, are presented. The effect of seismic activity is shown to play an extremely important role in the stability of lunar slopes and the indirect evaluation of lunar bearing capacity from studies of lunar slopes.

Using the data from trafficability studies made at the Waterways Experiment Station in Vicksburg, Miss., linear relationships were developed by G. L. Martin and W. A. Vischer expressing tire sinkage as a function of the contact pressure of the tire, the horizontal velocity of the tire and the cone index of the soil. The data were from tests of both rigid and pneumatic tires in sand and clay soil. The pneumatic tire tests, however, were the main source of the data. These relationships were developed in the summer of 1968, however more data were evaluated during the period from October 1, 1968 to September 30, 1969.

During the fall of 1968 and the summer of 1969, topographic maps of boulder tracks in the Hebgen Lake area were made in-place density and "static" bearing capacity (or bearing pressure) were recorded and soil samples were collected for laboratory classification. In talus material the size range of the particles and an approximate angle of repose was found. Samples of all boulders were taken for density measurements.

Using the above data a relationship is now being developed between boulder and soil properties and boulder movement. It is hoped that this can be correlated with the relationship already developed from the vehicle studies.

Penetration resistance estimates based on secondary impact craters (Contract R-66).--Values of the penetration resistance obtained by H. J. Moore from lunar secondary impact craters photographed by Lunar Orbiters II and III are comparable to or higher than those obtained by Surveyor spacecraft. Penetration resistances for about 115 secondary impact craters, computed

essentially as the ratio of the kinetic energy of the block to the volume of the crater, were compared with static bearing capacities for footings of the size of the boulder computed, using: (1) Terzaghi's bearing capacity equation, (2) a soil density of 1.35 g/cm^3, (3) a cohesion of 10^3 $dynes/cm^2$, (4) friction angles of 30, 35, and 40°, (5) crater depth for footing depth, and (6) dimensionsless numbers for general shear. Penetration resistances for about 66% of the sample exceeded the values for static bearing capacities when the friction angle was near 30°. The mean was near 35°. In computing penetration resistance, the ejection angle of the block is assumed to be 45° and the energy is corrected using the sine of the impact angle. A second method, using the Euler equation (corrected for the assumed angle of impact) and compared with static bearing capacities as above, indicated that 83% of the penetration resistances exceed the static bearing capacities for friction angles of 30°; the mean was near 36.5°. Use of Harry Nara's low velocity impact equation involving an inertial constant (near 1.0 g/cm^3 for sand) and the static bearing capacity yield mean friction angles near 34.4°. Finally, comparison of data on the penetration of concrete spheres (see section on experimental impact investigations) into sand show that the lunar surface materials compare well with terrestrial fine sand. For the terrestrial experiments:

$$K = \frac{mV^{0.7}}{2AP} = 179,$$

and for the Moon, the mean value of K is 290, and for about 70% of the lunar sample $K > 179$. In the equation, m is the block mass, V is the normal component of the block velocity assuming an ejection angle of 45°, A is the cross-sectional area of the block, P is the depth of the secondary crater, and K is a penetration parameter for a given set of projectile-target conditions.

Slope stability studies (Contract R-66).--A paper entitled "An Analytical Solution for the Stability of Finite Slopes" was written, and is now in the initial review stages. The development of an analytical approach to the finite slope stability problem was started in the paper. This method is similar to the method of slices in terms of the static analysis; however, exact integration is used for determining the actuating and resisting forces. An equation was derived expressing the safety factor of a homogeneous, finite earth slope in terms of the slope geometry, geometry of a circular failure arc, and soil parameters. Safety factors obtained from the derived equation, were compared with those obtained by methods currently in use. The equation for the safety factor was then differentiated, with respect to the radius of the failure arc, in a futile attempt to derive an analytical expression for the radius that yields the minimum factor of safety for any given center. Results of the differentiated expression and the basic expression were compared. This comparison showed that when the differentiated expression was nearly satisfied, the center yielding the minimum safety factor was also defined. The attempt to develop a completely analytical solution, solving explicitly for either the minimum factor of safety, or the radius associated with the minimum factor of safety, was unsuccessful. The study, however, successfully established correct analytical expressions for the actuating and resisting forces and results from these expressions compare favorably with the numerical integration methods presently in use.

Photogrammetry and Photoclinometry

Apollo Photogrammetry.--During contract year 1967 photogrammetrists under S. S. C. Wu produced a total of 14 contour maps of selected parts of the lunar surface (ranging in scale from 1:10 to 1:200,000), and 40 topographic profiles within the areas mapped. Photogrammetric models from Apollo missions 8, 10, and 11 were used. This work was done in support of Lunar Terrain Analysis and Trafficability (Contract W-12,388), and Apollo Site Investigations (Contract T-66353G).

Orbital Photogrammetry.--From models of Lunar Orbiter photographs, missions II, III, and V, about 60 topographic profiles were measured. This work was in support of engineering-geologic investigations of boulder tracks (Contract R-66), Apollo Site Investigations (Contract T-66353G), Traverse Research (Contract R-09-020-041), and also in support of mission planning studies within the Branch of Surface Planetary Exploration.

Other activities.--To increase the capability of the AP/C analytical plotter, it has been decided to connect the AP/C computer to the IBM-360 computer located at the Center of Astrogeology in Flagstaff, Arizona. Both the logic and circuit designs for the interfacing are in progress. Development of the software part, such as the assembler link program, is also underway. After the completion of this interface, the IBM 360 computer can be used for input/output, for program transfering and storage, for table look-up, and as a real-time computer for the AP/C plotter.

A detail topographic map of the Gosses Bluff area, Australia, was prepared for D. J. Milton, who is investigating this impact structure under the Impact Investigations program (R-66).

Photometric slope investigations (Contract T-66353 G).--Work by B. K. Lucchitta and associates on Lunar Orbiter II and III photographs has shown that only about 53 percent of Mission II first generation negatives were suitable for photometric slope derivation. An additional 12 percent of the negatives were considered usable, while the remaining 35 percent were unsuitable. Of the Mission III photographs about 72 percent of the framelets were acceptable, an additional 21 percent might be acceptable, and only 7 percent were unusable for photometric slope studies. Similar limitations apply to Lunar Orbiter I, IV, and V framelets, but these were not specifically tested.

Apollo 8 and 10 vertical steropair photographs presented an opportunity to compare lunar slopes derived photometrically with the same slopes derived photogrammetrically. To accomplish this 15 parallel scans were run on a Joyce-Loebl microdensitometer on an Apollo 8 frame and an Apollo 10 frame. The scanned area

encompassed 160mm^2. The coded density data were stored on magnetic tape and then processed digitally on the IBM-360/30 computer. The resulting slope values were plotted as X-Y profiles on the XYZ plotter and were then compared with three photogrammetric profiles of the same area. The Apollo 8 data showed agreement in one scan between the two methods. Small features of the other two scans agreed but the overall photometric elevations diverged somewhat from the photogrammetric data. Since the image chosen in this case was a crater rim, albedo variations in the rim material most likely affected the slope value calculations. Additionally each scan starts at a relative zero elevation and heights are integrated over the entire length of the scan. Errors are therefore cumulative, and contribute to the inaccuracy.

The Apollo 10 data showed agreement, in the major topographic features, between the two methods. The crater Moltke was clearly represented in the photometric profiles. These profiles indicated a depth of approximately 1200 m compared with a value of 1500 m obtained photogrammetrically. Another result of this study was the confirmation that albedo changes affect photometric profiles. This was obvious in slope changes resulting from the bright halo immediately around the crater Moltke. The effect was also demonstrated in slope changes across the landing site IIP-6-1, resulting from the light rays crossing the area.

Sources of errors in the slope values may be attributed to the following: (1) Inaccuracies in the geometric data relating the position of the Apollo spacecraft, the sun, and the lunar surface. These inaccuracies are due largely to the hand-held camera method and could be corrected through the use of a precisely aimed gimbal-mounted camera. (2) Albedo changes in the scanned area. (3) Inaccuracies in the lunar photometric function. (4) Density to brightness conversion errors. (5) Optical and electronic noise in the scanning system apparatus. Modifications now in progress will greatly reduce the optical and electronic sources of error.

Advantages of Apollo photography over Lunar Orbiter photography for purposes of slope derivation include: one piece, unmosaicked

frame format, sensitometric calibration of a suite of pictures rather than for individual framelets, and the lack of density variations introduced by the transmission and reconstruction of the images from the Orbiter spacecraft film.

The maximum vertical resolution of photometrically derived slope profiles of the Apollo 8 frame AS8-12-2082 (scale 1:375,000) was analyzed on a purely geometric basis. Because of the inherent errors in the method described, this resolution is a theoretical maximum and cannot be practically obtained. This value is approximately 1 m for slopes of 1°, 7 m for slopes below 5°, 26 m for slopes below 20°, and 43 m for slopes below 30°. The Apollo 8 frame analyzed had photometrically derived slopes below 20 degrees.

A preliminary investigation of the influence of albedo variations on photometric slope values was conducted. An area showing a mare surface with a small, symmetrical crater (Sabine E) was selected and several profiles were made using a different value for the albedo in each case. The results showed that adjustments in albedo values would not yield an accurate crater portrayal. If the slopes on the crater walls were similar, the center of the crater (0° slope) was shifted toward one side resulting in an asymmetric shape. Adjustment of the albedo to place the point of 0° slope in the center of the crater profile caused dissimilar slopes on the sides, again resulting in a skewed crater shape. An investigation into the cause for these errors is planned for the future.

PART B. CRATER INVESTIGATIONS

Natural Impact Craters
(Contract R-66)

Studies of four natural impact structures (Sierra Madera, Flynn Creek, Gosses Bluff, and Decaturville) are in progress or awaiting publication. Together with the earlier studies of the smaller craters, such as Meteor Crater, Ariz., and the Henbury craters, Australia, these cover most of the size range of the known terrestrial impact craters, except the largest ones such as Manicouagan, Sudbury and Vredefort.

Sierra Madera, Texas.--The final report on the geology of the Sierra Madera structure by H. G. Wilshire, T. W. Offield, K. A. Howard, and D. Cummings is in process of publication as a U. S. Geological Survey Professional Paper. Below is the abstract from this paper.

> The Sierra Madera structure is a bowl-or funnel-shaped body, about 8 miles in diameter and 6,000 to 8,000 feet deep, of intensely deformed sedimentary rocks, located at the southern edge of the Val Verde basin in west Texas. The deformed rocks are Permian and Lower Cretaceous shelf-facies carbonate strata. The structure is composed of three main parts: a central uplift, about 5 miles across, in which the oldest rocks have been raised 4,000 feet above their normal position; a surrounding structural depression, about ½ to 1 mile wide, that is floored mainly by Lower Cretaceous strata; and a concentric structurally high rim, about half a mile wide, in which Lower Cretaceous rocks are locally folded and cut by concentric normal faults downthrown toward the center.
>
> The intensity of folding and faulting increases inward from the flanks of the central uplift toward a central zone about a mile in diameter where dips and fold plunges are near vertical or overturned. Individual beds are repeated by folding and faulting so that their total strike length is greater than the length of the perimeter on which they lie, indicating both inward and upward movement of the strata forming the uplift. This movement pattern is substantiated by a thickened section in the center where only 1,200 feet of the oldest strata with generally steep dips fill an area with a minimum width of a mile. Drill data show that this thickening is not the result of domical arching of the oldest beds, but rather that it is a product or repetition of beds caused by centripetal movement.

The structural depression probably resulted from tectonic thinning accompanying the inward movement of rocks to form the central uplift. Folding and uplift in the outer rim may have been produced by outward-directed compression early in the deformational event.

Monolithologic and mixed breccias, shatter cones, and certain types of internal structures of minerals at Sierra Madera are ascribed to shock deformation. Monolithologic breccias, composed of shattered but unmixed rocks, are abundant on the central uplift. Generally the minerals in them show few signs of shock deformation, but there are indications that some shatter cones formed concurrently. Shatter cones, when the beds containing them are restored to horizontal, point inward and upward above the center of the structure. Mixed breccias form intrusive bodies in which fragments from beds as much as 1,700 feet apart occur together. Quartz grains in the mixed breccias have multiple planar elements and cleavages, dominantly parallel to $\{0001\}$, $\{10\bar{1}3\}$, $\{10\bar{1}2\}$, $\{10\bar{1}1\}$, and $\{10\bar{1}0\}$, and abnormally low refractive indices that indicate peak pressures above 200 kb. Planar elements in quartz from rocks still in place near the center of the structure record pressures above 100 kb, and those in quartz from rocks on the flanks of the uplift record pressures near 50 kb.

The symmetry of restored shatter cone orientations suggests that the cones were formed by a shock wave of generally hemispherical form that originated above the present ground surface over the center of the structure. As the shock wave traveled downward and outward from the central focus, the shock intensity progressively decreased. The only reasonable explanation of these conditions is surface impact of an extraterrestrial body. This interpretation is supported by the uniqueness of Sierra Madera in an otherwise normal geologic environment, its lack of relation to any regional or local structure, and the geometry of the central uplift which could not have been produced by a deep subsurface explosive event.

Although the mechanics of formation of the central uplift are still not completely understood, its structure is similar to uplifts in craters formed by surface detonation of TNT in Canadian cratering experiments. Analogy with experimental craters and with other crypto-explosion structures indicates that the uplift at Sierra Madera protruded into a crater, since destroyed by erosion, that was about 8 miles in diameter. Inasmuch as the rocks forming such uplifts are derived from below the crater floors, analogous lunar craters potentially offer

samples of lunar crust uplifted from distances below the crater floor on the order of one tenth the crater diameter.

Flynn Creek.--The manuscript on the geology of the Flynn Creek Crater, Tennessee, has been reviewed and the final illustrations and revisions are being completed. The paper will be submitted early in 1970 for publication as a U. S. Geological Survey Professional Paper.

Gosses Bluff impact structure.--A brief field season in 1969 by D. J. Milton was devoted to geologic study of the outer zones of the Gosses Bluff structure and to liaison with the geophysical parties of the Bureau of Mineral Resources of Australia. Early results indicate a slightly smaller but less deeply eroded crater than had been envisioned. More or less uniformly vertical outward-facing strata occupy a circular area 9-1/2 to 10 miles in diameter, which approximates the area within the rim crest of the former crater. Severely disturbed strata are found as far as two miles beyond this limit in some sectors, but these are in sharply delimited thin plates, as shown by geologic mapping and seismic refraction. These are apparently remnants of the rim of the crater, where shallow outward thrusting dominates. Seismic reflection indicates undisturbed strata at about 17,500 feet depth beneath the center of the structure and suggest that the beds now cropping out in the center of the Bluff have been uplifted about 11,500 feet.

Additional occurrences of thermally metamorphosed breccia were found around the Bluff. These are commonly obscure on the ground but are clearly marked by aeromagnetic anomalies. Their distribution suggests that the plain around the Bluff is a stripped surface approximating the base of the shocked breccia. One particularly significant outcrop lies at the very base of the outer Bluff wall, which indicates that the present Bluff is not merely an erosional feature but was a central peak buried to an unknown depth by melt breccia.

These findings allow the pre-erosion form of the crater to be recovered more closely than was expected. The geologic mapping and particularly the shatter cone data together with the seismic and

gravity data on the subsurface allow determination of the displacement vectors in the central uplift zone. Thus both the structural and morphologic development of the crater can be reconstructed more closely than anticipated.

The seismic, gravity, and magnetic studies being carried out by the Bureau of Mineral Resources are certainly the most thoroughly integrated geophysical campaign that has been carried out at any impact structure,-- perhaps even at any geologic structure regardless of origin.

Seismic work occupied a thirty man party for eighteen weeks. Continuous reflection profiles were shot over two 16-mile traverses crossing at right angles in the center of the Bluff. Common depth point multiple stacking was used over most of the length, up to 24-fold stacking inside the Bluff itself. On one of the arms controlled directional reception was used to detect the steep dips within the disturbed zone. This technique, recently developed in the USSR, utilizes shot delays in an extensive shot hole array to produce an oblique wave front. A downhole velocity log run at Magellan Petroleum's Tyler No. 1 well (just completed as a dry hole at 12,599' T.D.) close to the end of one of the traverses, and several extended spreads yield velocity data. A special shallow refraction traverse was shot over known geology within the disturbed zone and first breaks are being analyzed on the long traverses.

Gravity has been measured with a Lacoste-Romberg gravimeter at stations spaced every quarter mile over a four mile square grid, every half mile over a fifteen mile square grid, and on more closely spaced traverses over special geologic features. There is a negative anomaly of about 5 milligals associated with the structure as a whole; considerable detail within the structure remains to be analyzed.

Magnetic mapping was carried out by low level flight in radial traverses. There is no anomaly associated with the structure as a whole, but numerous local anomalies were detected. Milton was able

to attribute virtually every one of these to melt breccia or thermally metamorphosed breccia. Two of the anomalies were mapped in detail by a ground magnetic party. The BMR geophysicists fitted a dipole to the Mt. Pyroclast anomaly as indicated on the aeromagnetic record and concluded that it had an inverse orientation with an inclination of 80°, presumably theremoremanent magnetization induced by the Earth's field at the time of impact. This may be compared with a 72° inverse inclination actually measured in the Menlo Park Laboratory on drill core from Mt. Pyroclast. This season oriented core was obtained so that the declination can be measured as well.

Computer analysis of the shatter cone data collected in 1968 (with a few additional measurements in 1969) is complete. Out of 95 shatter cone stations measured, 87 yielded cones of sufficient quality for use in the orientation programs. If the beds are restored to horizontal at elevations appropriate to their stratigraphic position, the cone axes point to a focal zone above the center of the Bluff. The foci of cones in different stratigraphic units are spread vertically within this zone.

The simplest interpretation of the spread is that it is a result of the increasing inward as well as upward displacement of the rocks from the outside of the structure to the center, and in fact may be used to measure the inward displacement.

Two independent dating methods indicate an Early Cretaceous age for the Gosses Bluff event. A K/Ar date of 133 ± 3 m.y. was measured on a specimen of sanidine-rich pumice that forms one of the minor rock types in the Mt. Pyroclast melt breccia (R. Marvin, Branch of Isotope Geology). Fission track dating of annealing in zircon and apatite from baked breccia recovered from drill holes beneath the melt breccia is still in progress, but a preliminary date of about 120 m.y. is currently indicated (C.W. Naeser and D. J. Milton). Aside from the significance for Gosses Bluff itself, this provides one of the few reference points, either absolute or stratigraphic, in the Mesozoic history of central Australia.

Petrographic study of the highly shocked breccia indicates transformation to noncrystalline phases (probably including both truly melted rocks and glasses produced by shock at subsolidus temperatures) followed by a period of recrystallization at high temperatures, as might be expected at the base of the melt breccia zone. Much of the free silica crystallized as tridymite (since inverted back to quartz); high-temperature sanidine and several zeolites (heulandite, chabazite, and stilbite) also formed. Processes during the stage of recrystallization were not entirely isochemical. For example, most of the 12.6 percent of K_2O in the material used for dating must have been acquired from aqueous solutions rather than having been present in the shale precursor. This is of significance in relation to the Canadian cryptoexplosion structures, where high potash contents have been brought forward as evidence for alkalic volcanism rather than melting of country rock by impact.

Decaturville, Missouri.--Approximately half of the Decaturville cryptoexplosion structure was mapped during FY 1969 by T. W. Offield and H. A. Pohn. Much of the field work was devoted to identifying rock units and establishing the stratigraphic section in detail, a difficult task because the structure exposes formations not seen at the surface elsewhere in central Missouri, and correlation with distant sections is tenuous because of facies changes and extreme brecciation.

The structure, about 3-1/2 miles in diameter, consists of a central uplift surrounded by a structurally depressed ring zone delimited by an approximately circular boundary fault. At least 1800 feet of section is disturbed. The youngest rock in the structure is Silurian Bainbridge Limestone; the structure is at least younger than that unit. Other rocks preserved in the down-dropped ring zone are the Kimmswick Limestone and about 150 feet of Jefferson City Formation of Ordovician age. Fossils collected from the Kimmswick include ammodiscids not previously known from the Ordovician. The Jefferson City has been subdivided in detail in order to study the geometry of deformation in the ring zone.

Exposures in this zone are better than in analogous zones around other cryptoexplosion structures examined so far. The Cambrian Derby-Doerun Formation underlies the center of the uplift, with the Cambrian Potosi and Eminence Formations and the Ordovician Gunter, Gasconade, and Roubidoux Formations forming circular outcrop zones progressively outward around it toward the ring zone. Isolated blocks of deeper formations (Davis, Bonneterre, Lamotte, and Precambrian pegmatite and schist) have been brought to the surface by faulting. Study of about 18,000 feet of cores available from many holes at the center of the uplift shows extreme disruption of beds in the subsurface, with juxtaposition of formations involving upward and downward movements of several hundred feet.

Shock is probably indicated by shatter cones and by the unusual type of monomict breccias also seen in several other cryptoexplosion structures believed to have formed by impact. Shatter cones are moderately well developed in the Derby-Doerun Formation within about 1,500 feet of the center of the structure, but their orientations cannot be analyzed until a way is found to determine bedding attitude in the massive dolomite host rock. Monomict brecciation is characteristic of every carbonate formation in the structure and together with other deformation ends abruptly at the boundary fault. The intense small scale deformation may have taken place momentarily after the major displacement represented by the central uplift and the boundary fault. Quartz grains in the Gunter Sandstone, which rings the structure about 1/3 mile from the center, consistently show rectilinear mosaic structure under the microscope. At least two sets of sparse planar features are seen in quartz of Lamotte Sandstone blocks several hundred feet above the normal stratigraphic position of the Lamotte. These planar features have not yet been confirmed as shock lamellae, however,

A geophysical survey shows that the central uplift is a slight gravity high and the whole structure is a magnetic low. Detailed gravimeter and magnetometer traverses in the center, where traces

of mineralization are seen at the surface, revealed no anomalies which might indicate subsurface ore bodies. A magnetic anomaly inside the boundary fault is believed to mark the intersection of the fault with crystalline basement rocks. The fault apparently has an average dip toward the center of about 45 degrees, but as it is steeper than this at the surface it is probably curved so that it intersects the basement at a low angle, giving a bowl-like configuration to the boundary surface of the structure.

Impact Metamorphism
(Contract R-66)

Detailed optical studies by E. C. T. Chao of quartz from granodiorite of the Ries Crater showing various degrees of shock were continued. Interference microscopy was used to measure the refractive index of shock lamellae as compared to the host fragment in order to estimate the amount of glassy phase present. The same oriented fragment was then transferred with a specially designed device to be mounted on a goniometer head for x-ray single crystal study. The x-ray studies showed that it is potentially possible to detect shock effects on the basis of intensity changes of certain reflections related to the crystallographic orientation of the shock lamellae. The detection limit seems more sensitive than that of optical microscopy. This is a part of the long range detailed study of the classification, determination of various types of microstructures of shock origin and the mechanism of slip, defect structure, disordering and phase transition. Correlation of the nature of the microstructures with the peak shock pressure and induced temperature instrumental in their formation is anticipated. This is of joint interest between the experimental shock phase study project and the impact metamorphism project.

Detailed shock-produced textures are being studied and described for a series of crystalline rocks and glasses. This basic information will be useful in distinguishing shock-produced textures from igneous textures. Full knowledge of the pre-shocked

and shocked rock in textures and mineralogical composition is basic toward understanding of the origin of lunar material.

Basic criteria of shock and information for their proper interpretation, developed and established by investigations conducted under this project for the past nine years have been found to be directly applicable to the study of lunar samples returned by the Apollo 11 mission. The microstructures of shock origin, the occurrence of thetomorphic mineral glass and the formation of glass spherules containing clouds of nickel-iron are examples widely exhibited by the Apollo 11 samples. It is gratifying that we are prepared in this respect for the study of returned lunar samples. Experimental shock phase study and the detailed study of the interaction of shock wave with mineral phases should be vigorously pursued and extended to the study of complex histories where multiple shock events are involved.

Shock phase studies.--Research by O. B. James during the contract year has been directed toward establishing criteria diagnostic of shock metamorphism as a continuation of the previous studies of impact metamorphism. Transformations diagnostic of shock have been found in plagioclase and olivine, two common rock-forming minerals. In amphibolites from the Ries Crater, jadeite (high pressure Na-Al pyroxene) formed by shock-induced breakdown of sodic plagioclase. In basalts from a crater produced by a nuclear explosion at the Nevada Test Site, distinctive lamellar structures were formed by shock in olivine. These structures consist of sets of narrow, subparallel planar bands of alternating high and low indices of refraction. Commonly more than one set is developed per grain, and the sets have associated mosaic extinction.

To provide a basis for comparison with the returned lunar samples, detailed studies are being made of the shock and thermal metamorphism of basalt by nuclear explosion. Metamorphosed basalts have been classified into five categories: (1) Weak. All minerals are strongly fractured, show weak intragranular deformation (twinning in augite, undulatory extinction and possible deformation

lamellae in olivine); (2) Moderate. Plagioclase is converted to thetomorphic glass, olivine and augite show pronounced intragranular deformation, but rock texture is perfectly preserved; (3) Moderately strong. Feldspar glass shows small-scale flow, augite is minutely fractured, olivine is coarsely fragmented, and the mafic minerals show strong intragranular deformation; (4) Strong. Feldspar glass is vesicular, augite has strong undulatory extinction, mechanical twinning, and possible deformation lamellae, and olivine contains distinctive lamellar structures, and smooth undulatory extinction, banded extinction, or mosaic extinction; and (5) Intense. The rocks are converted to inhomogeneous basaltic glass.

D. J. Roddy, in cooperation with T. J. Ahrens, California Institute of Technology, has conducted experiments on single crystals of shock-loaded optically clear calcite. Pressures ranged from 5 to 30 kb. Lattice deformation indicated by x-ray line broadening has been found at pressures as low as 10 kb and becomes increasingly prominent in all crystal orientations at higher shock pressures. Petrofabric studies indicate a corresponding increase in the number of planar features accompanying the higher shock pressures. The type of deformation and the x-ray patterns are very similar to those observed in calcite from impact sites. Shock pressure at the natural sites, inferred from the experimental work, are generally consistent with available theoretical hydrodynamic data from computer studies on rock systems.

Volcanic Studies
(Contract R-66)

Projects dealing with volcanic craters include studies of roots of maar craters, morphology of craters formed in basalts of different types, and a caldera in a basalt shield. Other volcanic studies include the investigation of: 1) lava tubes at South Prairie, Idaho, and at the Modoc field, Lava Beds National Monument, Calif., 2) volcanic domes at Mono Craters, Calif., and in southwestern New Mexico, and 3) a variety of volcanic landforms at the Diamond Crater complex in southeastern Oregon. A map of the Mule Ear diatreme, Utah, and reports on the Lunar Crater chain of basalt craters,

Nev., and the Fernandina caldera, Galapagos Islands, are in process of publication. Field work was concluded at Nunivak, Alaska, Lava Beds National Monument, Smith Prairie, and the two areas of rhyolite domes; final reports are in preparation. Active study of the San Francisco volcanic field in northern Arizona was temporarily postponed.

Lunar Crater volcanic field.--Work by D. H. Scott and N. J. Trask on a U. S. Geological Survey Professional Paper chapter devoted to the Lunar Crater volcanic field, Nye County, Nev., was nearly completed during the past year. An abstract of the report in its present form follows.

> The Lunar Crater volcanic field in east central Nevada includes cinder cones, maars and basalt flows of probable Quaternary age that individually and as a group resemble some features on the Moon. Three episodes of volcanism are separated by intervals of relative dormancy and erosion. Changes in morphology of cinder cones, degree of weathering, and superposition of associated basalt flows provide a basis for determining the relative ages of the cones. A method has been devised whereby cone heights, base radii, and angles of slope are used to determine semiquantitatively age relationships of some cinder cones.
>
> Structural studies show that cone and crater chains, with associated lava flows, developed along fissures and normal faults produced by tensional stress. The petrography of basalts and pyroclastics suggests magmatic differentiation in flows of older to intermediate age and a mantle origin for ultramafic xenoliths in the younger basalts and ejecta.
>
> All of the features in the Lunar Crater volcanic field have analogs on the Moon. Features on the Moon interpreted as maars may have details of structure and composition similar to Lunar Crater itself. Erosion on the Moon, probably caused by the impact of small particles and attendant downslope slumping of the material, appears to be grossly similar to the erosion of the cinder cones in the Lunar Crater volcanic field where removal of material by streams is at a minimum.

A preliminary report on ultramafic xenoliths which occur around two of the vents in the Lunar Crater volcanic field was completed by N. J. Trask (1969). An abstract of that report follows.

Lherzolites from ejecta and flows around two vents in central Nevada are moderately to strongly deformed; olivine-rich wehrlites and dunites are intensely deformed; and clinopyroxene-rich wehrlites, clinopyroxenites and gabbros are undeformed to only slightly deformed. The olivine-rich wehrlites contain striking large, black, glassy clinopyroxene grains some of which are broken and invaded by fine-grained recrystallized olivine. The lherzolite probably came from the upper mantle; the clinopyroxene-rich wehrlite, and clinopyroxenite may have formed in the lower crust as cumulates from the magma that produced some nearby basalt flows older than the host rock; source of the highly deformed olivine-rich wehrlite and dunite is not clear.

Fernandina caldera.--The 1-2 km^3 enlargement of Fernandina caldera, Galapagos Islands, in June, 1968, ranks it among the largest historic collapses. Study of the caldera geometry, together with eyewitness reports, serves as a basis for interpreting geophysical signals received by distant stations. The study is being conducted jointly by K. A. Howard and R. E. Simkin, Smithsonian Institution.

Two weeks of high seismic activity accompanied the collapse. The total energy of the seismic swarm, 5×10^{19} ergs, was greatly exceeded by the potential energy of the collapse ($> 10^{23}$ ergs), so the earthquakes probably formed by frictional displacement as the caldera floor was lowered as much as 300 m along its elliptical boundary fault. The chronology and energetics will be further refined through study of distant hydrophone records, which show about twice as many events as reported from conventional seismic records.

Explosions preceding the collapse furnished more energy ($> 10^{21}$ ergs) than the earthquakes, and built an ash cloud 20 km high and hundreds of kilometers long. The source may be a new explosion crater, only 50 m wide, on the floor of the caldera. The volume of erupted products is however many times smaller than the volume of collapse, so magma must have been withdrawn at depth to provide room. The removal of this material probably unloaded the center of the volcanic pile, so that rapid uplift due to isostatic readjustment may now be occurring. If properly monitored,

Fernandina would provide an unequaled opportunity for study of isostatic adjustments in large craters.

Bend, Oregon.--The Diamond Crater complex in southeastern Oregon is being studied by L. C. Rowan to determine the relationships between morphology of the volcanic landforms and their petrologic and structural history. A wide variety of well exposed, youthful volcanic landforms is exposed in this relatively small (6 miles in diameter) area.

The complex consists of alternating basaltic flows and tephra deposited on Pleistocene lake bed sediments and, on the east side of the area, on older rhyolite and basalt. Three main episodes of magmatic activity have been identified: the first involved doming along a northwest trending axis and extrusion of viscous basaltic magma from near the center of the dome; the second involved burial of these flows by ash and cinders; and the last, local extrusion of basaltic flows and construction of cinder cones. In addition, there appears to have been development of cinder craters and cones between the first and second stages. Of particular interest is the concentration of doming, extrusion of lava, and explosive activity along the northwest line. Evidence suggests that there may have been progressive movement of the center of activity from southeast to northwest as the complex developed. Older craters and cones were transected and covered, resulting in a wide range of morphologic types. The relationship between the mechanism of movement of the magma and its interaction with the older deposits and the resulting morphologic changes are now being investigated.

To better define the physical and chemical characteristics of the deposits and their relations with the morphology of the various craters, mechanical and chemical analyses are being made. It is anticipated that these investigations and refinement of the preliminary geologic map will be completed during FY 1970.

Mule Ear, Utah.--The detailed geologic map of the Mule Ear diatreme, by D. E. Stuart-Alexander, E. M. Shoemaker, and H. J. Moore, was submitted for publication. Salient aspects of the geology of this feature are summarized below.

The Mule Ear diatreme at its present exposure level contains a mixture of blocks of sedimentary rocks that have been displaced downward, some more than 5,000 feet, and basement-complex xenoliths that have been transported upward, some probably tens of thousands of feet. In plan the diatreme is crudely zoned into a thick outer zone of dominantly down-dropped blocks of sedimentary rocks, an irregular middle zone of reconstituted clastic sedimentary materials with minor admixed debris from igneous and metamorphic rocks, and an inner core of uplifted xenoliths and pulverized debris that may be altered foreign igneous material or altered material related to the diatreme.

The crude zoning of the rocks probably reflects differences in the movement pattern within the diatreme. Stoping seems to have been the primary mechanism of enlarging the diatreme, loosening the blocks in the outer zone so that the larger blocks could be lowered as finer fragments were removed. Active disaggregation or comminution of the sedimentary rocks occurred in the middle zone, followed by limited mobilization and injection in the form of sandstone dikes. The strongest deformative forces and greatest distances of transportation took place in the innermost zone.

Minerals from two xenoliths of granite found at the Mule Ear diatreme were dated by the fission track technique by C. W. Naeser. Apatite and sphene were dated from one sample, and apatite was dated from the other. The apatite ages are 28 ± 3 m.y. and 30 ± 3 m.y. The sphene has an apparent fission track age of 690 ± 100 m.y., in contrast to the 1400- to 1800-m.y. age of its probable source rock. This shows that the inclusions have been heated causing annealing of the fossil tracks.

Fission tracks in apatite are annealed at relatively low temperatures, less than 350°C, while sphene requires higher temperatures. The apatite indicates that the diatreme cooled approximately 29 m.y. ago. Sphene on the other hand lost approximately 50 percent of its fossil tracks. Annealing studies on sphene indicate that the maximum temperature to which this granit xenolith had

been heated was between 300 and 500°C. The rock could have been heated during the intrusion of the diatreme, or it could have been brought up from a depth where the temperatures were sufficient to anneal fission tracks.

Moses Rock diatreme, Utah.--Electron microprobe investigations of minerals from Kimberlite and dense rock fragments in the Moses Rock diatreme were performed by T. R. McGetchin and L. T. Silver, California Institute of Technology. The results suggest equilibration at upper mantle pressures.

Field studies of fragment size of the sedimentary clasts in the diatreme show a decrease in size with distance of upward transport from original locations in the walls of the diatreme. This relationship, when applied to the crystalline fragment populations, provides an empirical basis for reconstructing the vertical stratigraphy of crystalline rocks in the crust and upper mantle. On the basis of size, abundance, and petrographic character, metabasalt, granite, and granite gneiss are abundant in the upper part of the crust along the dike walls; diorite, gabbro, and mafic amphibolite constitute intermediate crustal layers; and mafic granulite and possibly hydrated ultramafic rocks constitute the lower crust. The suite of crustal rocks in this area is thus predominantly meta-volcanic or metaplutonic,-- not metasedimentary.

Dense, ultramafic fragments (possibly mantle rocks) include antigorite-tremolite schist, jadeite-rich clinopyroxenite, eclogite, spinel websterite, and spinel lherzolite. The presence of garnet lherzolite is inferred from mineral inclusions observed in pyropic garnets.

The Mohorovičić discontinuity apparently occurs within a petrologically complex region and may coincide with phase and compositional transitions, including hydration. A compositional transition within the mantle between spinel and garnet peridotite (lherzolite) is consistent with observations. The variety and abundance of ultramafic and dense rock types, together with the complexity of their textures, suggest the mantle may be as complicated as the crust in

composition and history. It also seems likely that the upper mantle may contain a significant amount of volatile material (water and/or CO_2) at modest temperatures (possibly 950°C at a depth of about 150 km).

Titanium-rich clinohumite and layered structure minerals occur in kimberlite and as inclusions in pyropic garnets from the Moses Rock dike. The presence of titanoclinohumite, a high density hydrous phase, is of considerable interest because it suggests a possible source for volatiles in the Earth's upper mantle. The dehydration of hydrous phases such as titanoclinohumite within the upper mantle may provide water as a free phase.

Cane Valley, Utah.--The Cane Valley diatreme was investigated by T. R. McGetchin and a report was prepared. This structure is interesting because it is believed to be a kimberlite diatreme arrested in a very early stage of development, and also because coarse-grained intrusive carbonate with garnet and biotite (carbonatite?) is present.

Nunivak, Alaska.--K. J. Rohlof completed a study of the exterior ballistics of block ejecta at Nanwaksjiak crater, Alaska. Using field data collected by J. M. Hoare, T. R. McGetchin and Ivo Lucchitta, he estimated the mean properties of an erupting fluid capable of accelerating blocks of the observed size to sufficient velocity to attain the observed ballistic ranges. He included atmospheric drag, using a variable coefficient of drag. Blocks were ejected at greater than the speed of sound, and drag significantly affected the ballistic range of blocks more than 2 feet in diameter. Because the ejection angle is not known, these results are not unique. However, by using an estimated launch angle of 65 to 70° (based on available volcano photography), Rohlof estimates the erupting material at Nanwaksjiak to have had a velocity of 500 m/sec and a density of .01 gm/cc near the surface.

G. Wayne Ullrich extended previous work by McGetchin and constructed more than five hundred detailed numerical models for flow in hypothetical volcanoes in which the flow properties

(velocity, temperature, density, Mach number, Reynolds number, etc.) were calculated as various environmental parameters (such as gravity, duct shape, etc.). Ullrich includes frictional losses, expansion near the surface, and heat transfer between condensed particles and volatiles. The resulting surface properties of these models were compared with field observations for Nilahue (a Chilean volcano that erupted in 1955), Nanwaksjiak, and Moses Rock. Despite poor data on active volcanos, certain constraints can be placed on the models by field data such as block sizes thrown to various ranges (as at Nanwaksjiak) or the size of large blocks carried upward in diatremes (as at Moses Rock). These models suggest that surface eruption velocities are commonly of the order of several hundred meters per second (commonly Mach 2 to 4), and volatile temperatures are low at the surface. Flow velocities are modest at depth but become very significant near the surface. Dynamic pressure ($pu^2/2$) goes through a broad maximum at about 1 to 2 kilometers depth and hence the carrying capacity of the fluid is greatest near but below the surface.

Ullrich's calculations have been extended to the Moon, Mars, and Venus to evaluate the ejecta distribution around lunar and planetary diatremes. The surface velocity of entrained fragments of various sizes was calculated using Ullrich's computer models for the appropriate value of gravity. Exterior ballistic range was computed including the effect of atmospheric drag (using currently accepted values for planetary atmospheric properties). Major results are: (1) Very small ejecta from lunar diatremes may attain ballistic ranges of up to 250 kilometers, but larger ejecta have shorter ranges. (2) For planets with atmospheres, even as tenuous as the atmosphere of Mars, a reversal in range versus size is predicted; that is, large blocks go farther than small ones, which is consistent with ejecta ranges from atomic explosions and from the recent Taal and Arenal volcanic eruptions. The distribution of fine ejecta on planets with atmospheres is not determined by ballistics-- rather by atmospheric conditions (wind);

(3) Calculations suggest that very volatile-rich eruptions on the Moon (10% by weight volatiles) would attain surface velocites of approximately 580 m/sec, significantly less than lunar escape velocity. This implies a ballistic range of about 250 kilometers for ejection at 45°.

These results, combined with field observations of ultramafic and eclogitic fragments at Nanwaksjiak and Moses Rock, suggest some conclusions regarding lunar diatremes. Xenoliths in terrestrial occurrences commonly are found in the material ejected late in the eruption, as shown by their concentration near the top of the associated ash. Also these fragments are commonly about 10 cm in size. Calculations suggest that ejecta, especially the fine component, may be more widely distributed on the Moon than on the Earth. This in turn suggests that xenoliths will be more widely dispersed and less densely concentrated near the crater rim. Hence it may not be necessary to land very near a particular lunar diatreme in order to collect xenolithic material from it.

Lava tubes.--Geologic mapping at a scale of 1:5,000 has been completed by K. A. Howard on four lava tube systems in northern California. The tubes are as much as 17 km long, as much as 2,000 m^2 in cross-sectional area, and have gradients as low as 0.25°. Features indicative of flow direction found on tube walls should be of particular interest for manned exploration of lunar sinuous rilles. Some collapse trenches along the tubes are surrounded by blocky rims as high as 8 m. The rims are the steeply dipping to overturned flanks of anticlinal folds, the centers of which have collapsed into the underlying tube. Despite the non-explosive origin of the rims, they are commonly chaotic, include completely inverted blocks formed by outward toppling, and generally resemble ejecta.

Study of Pleistocene basalts along the South Fork Boise River, Idaho, established the stratigraphic order of six distinctive flows separated by erosional intervals. The youngest flow, at Smith Prairie, contains a lava tube in a narrow tongue that followed an

old creek channel. Large volumes of basalt passed through the tube and then cascaded into a Pleistocene river gorge, where sequences of pillow basalts that formed from damming of the river show promise for determining the lava flow rate through the tube. Changes in lava composition and texture that occurred during the eruption reflect the course of crystallization in the magma chamber.

Volcanic domes.--As part of a comparative study of terrestrial and lunar volcanic domes, Eugene I. Smith mapped a Pliocene dome complex in southwestern New Mexico and a small double-ring structure in the Mono Craters area, California. Research is also being conducted to develop criteria for the recognition of volcanic domes on the lunar surface and to determine the distribution of lunar domes.

The John Kerr latite dome complex, N. Mex., is composed of three morphologically different extrusions. The western portion of the complex is occupied by a large (5 km diameter) subcircular, convex upward, lens-shaped body. Foliation is concentric with the margins of the body and dips moderately outward. Overlying and completely encircling the dome is a thick accumulation of laharic and waterlaid monomict breccia. In places toward the western margin, monomict breccia is found surrounding spines of massive latite and filling depressions. The relationship with underlying massive latite suggests that this debris is primary carapace. A plug of latite with steeply dipping north-south striking foliation is located to the east of the lens-shaped body. The western flank of this structure is covered to the summit by unsorted, unbedded monomict breccia, interpreted as original and reworked carapace. The structure probably was extruded from a north-south trending fracture. One kilometer to the east of the plug is a funnel-shaped body intruding a series of flat lying latite flows. This combination probably had the appearance of a terraced dome (dome and coulee) soon after extrusion. Each dome type has an analog on the lunar surface.

The double-ring structure mapped in the Mono Craters, California, is located to the south of the Southern Coulee. The double

ring (diameter 900 m) is composed of a cratered parasitic dome occupying the central portion of an explosion crater of an older dome. The structure of both domes is funnel shaped. This body may be an analog to small double craters on the lunar surface.

A survey of Lunar Orbiter photographs for volcanic morphologies has been completed. Over 200 previously unreported volcanic constructional features have been recorded.

Missile Impact Craters
(Contract R-66)

Four missile impact craters were mapped (data tabulated below) and passive seismic studies were continued during FY 1969.

Target	Target Density (g/cm^3)	Kinetic Energy (10^{14} ergs)	Impact Angle	Rim Diameter (Meters)
1. Sand, weakly cohesive	1.6	69.9	40°	7.4
2. Alluvium gypsiferous	1.58	13.5	52°	4.0
3. Alluvium, gypsiferous	1.58	14.5	52°	4.0
4. Sand, very weakly cohesive, gypsum	1.4	73.5	35°1/	10.0

1/ Does not include slope of dune surface which is approximately 20°, making the impact angle about 55°.

Four missile impacts were used to obtain data on the seismic waves generated by impact (only two of the craters were mapped) as part of the ALSEP program. Four successful tests, conducted by Drs. G. V. Latham and W. McDonald of Lamont Geological Observatory, were completed using new light-weight equipment. The results from these tests will be used when the Lunar Module and Saturn IV-B are impacted on the lunar surface during Apollo 12 and subsequent missions.

No mapping of craters is planned until late 1970 when craters produced by higher energy projectiles will be available.

It is planned to write an article summarizing the data on missile impacts and comparing these data with other data on experimental impact during the coming year.

Experimental Impact Investigations
(Contract R-66)

Impacts in sand.--Studies of 22 vertical impacts of large concrete spheres at velocities between 1.0 and 10.8 meters/sec with fine sand were conducted. Sphere diameters were 9.44 cm, 16.30 cm, and 21.40 cm and densities were 2.31 g/cm^3, 2.30 g/cm^3, and 2.04 g/cm^3 respectively. It was found that:

$$\frac{mV^{0.7}}{2\,AP} = 179\ (\pm\ 15\%)\ \text{cgs units} \qquad (1)$$

where: m is the projectile mass,
V is the projectile velocity,
A is the cross-sectional area of the sphere,
P is the depth of penetration.

and

$$\frac{\frac{1}{2}\,mV^2}{\frac{m}{A}\,\text{Vol}\,V^{0.8}} = 380\ (\pm\ 15\%)\ \text{cgs units} \qquad (2)$$

where: Vol is the crater volume.

Water drop craters.--A study of transient craters produced by water drops falling on water was completed and will be published soon. The abstract of that paper follows:

> Studies of transient craters in water produced by falling water drops show that significant amounts of energy are present as kinetic energy in a cylindrical wave which surrounds the crater when the crater has reached its maximum size. At maximum size, about 80 to 90 percent of the initial drop kinetic energy can be accounted for as potential energy, surface energy, and kinetic energy of the outwardly expanding cylindrical wave. The energy partitioning changes with

velocity and crater size. For 14 milligram drops with velocities near 155 cm/sec, surface energy is the most important energy sink; whereas potential energy is the most important energy sink at velocities near 566 cm/sec. The percentage of kinetic energy in the cylindrical wave increases with increasing drop velocity and may exceed that of surface energy for the highest velocities.

Explosion Crater Investigations
(Contract R-66, in part)

Chemical explosion craters in alluvium at the Defence Research Establishment, Suffield, Alberta, Canada, and in hard rock at the Cedar City, Utah, test site are being studied by D. J. Roddy in terms of basic cratering mechanics and their relationship to large scale impact cratering processes.

Prairie Flat Crater.--Detonation in 1968 of a 500-ton TNT sphere tangent to the ground surface produced a crater in alluvium 60 m in diameter and 5 m deep. Surface studies and excavations have shown that the topographic and structural configuration are similar to those of certain large terrestrial impact craters. The crater has a broad, flat central uplift, concentric ring folds on the crater floor, limited rim folding accompanied by high-angle faults, and a continuous ejecta blanket.

Excavation of the inner rim showed the original ground surface to be faulted en échelon with low-angle thrust blocks being moved outward as much as 2 m; the original ground surface now dips 20° to 30° in towards the crater.

A large overturned flap overlies the rim and contains continuous units of interbedded sand and clay lying in an inverted position. The overturned flap extends out as far as one crater diameter (61 m) as a hummocky unit. Brittle fracture and radial separation of individual clay beds on top of the overturned flap produce narrow, discontinuous, concentric ridges that give a topographic effect similar to that seen around the younger, large lunar craters, such as Tycho. The fractures and radial separation in the rim occurred during the dynamic overfolding.

Asymmetric extensions in the air shockwave and fireball produced by the detonation have been correlated in position with asymmetric extensions in the crater ray ejecta pattern and foldback. These correlations indicate initial inhomogeneities in the fireball and in the transmission of the shockwave to the ground. Apparently the inhomogeneities in the shockwave were primarily responsible for the patterns of rays in the ejecta and of asymmetric distribution of the foldback. No base surge deposits were positively identified.

Clay particles were fused below the TNT charge and were distributed as fallout over the crater, ejecta blanket and surrounding area. A series of x-ray fluorescence analyses have been completed on these fused fragments and each appears to have been derived from the upper 1 to 2 meters of soil below the TNT charge. Petrographic studies have confirmed that thermal effects ranged from baking and incipient surface fusion of individual soil fragments to complete fusion and intense vesiculation. Both the chemical composition and petrography indicate similarities with impactite material. A series of disequilibrium, high-temperature fusion experiments have been completed on undisturbed soil fragments; minimum fusion temperatures indicated by these experiments suggest soil disequilibrium temperatures at the time of detonation were in excess of 1100°C and probably on the order of 1500°C. Further tests are in progress.

Excavation of the crater floor and deep crater rim were completed in 1969 and show a general uplift in the form of concentric anticlines below much of the crater floor. Pronounced anticlinal development occurs below the crater walls with some beds overturned. The central part of the crater floor contains a broad, flat central uplift with beds raised at least 5 m.

A topographic map of the Prairie Flat 500-ton TNT crater has been compiled by the USGS in Flagstaff at a scale of 1:500 and a contour interval of 0.25 m. A final report is being prepared for publication by the U. S. Geological Survey.

AN/FO Crater.--The U. S. Defense Atomic Support Agency and the Canadian Defence Research Establishment detonated a 100-ton hemispherical charge over alluvium and lying on the ground surface at the DRES test site in Alberta, Canada. D. J. Roddy, with a U. S. Geological Survey Beaver aircraft, completed air blast, oblique and low altitude black and white and color photography of this cratering experiment. The crater, 46 m in diameter and 9 m deep, had a raised rim, overturned flap, terraced rimcrest, and a hummocky ejecta blanket with inverted stratigraphy. Deep excavations through the crater showed sharp anticlinal folds under the rims. A central uplift was not formed, apparently because the groundwater table and water-saturated clay layers were several meters deeper than at previous crater experiments which did have central uplifts. Data reduction of velocity and acceleration gages is now in progress and a geologic map and report are being prepared.

The topographic configuration of this crater is very similar to the smaller, fresh bowl-shaped craters seen on the lunar maria.

Mine Shaft Crater (1968) Series.--Two 100-ton TNT spheres and some smaller charges were detonated at the Cedar City, Utah, test site by the Waterways Experiment Station under the direction of the Defense Atomic Support Agency. The objective was to study craters and ground shock effects on hard rock surfaces (tonalite). The first 100-ton shot was detonated about 5 m above ground and produced a breccia mound about 1 m in height and about 10 m in diameter. The second was buried about 0.25 m (center about 2.2 m above ground) and produced a crater about 14 m in diameter and 3 m deep. A blocky ejecta blanket with a prominent ray pattern was formed; one ray was 21.5 times the crater diameter in length (300 m).

Well-developed shatter cones were produced in the tonalite. The largest crater having shatter cones, the 14 m diameter crater described above, had several ejecta blocks (up to 1.0 m across) which exhibited typical conical fracture surfaces of shatter cones with parasitic nests of cone segments up to 0.5 m long. One of the smaller craters, 2.4 m across and 0.33 m deep, was formed by

a 1,000-lb TNT sphere buried 0.04 m (center 0.37 m above ground). Striations on a complete shatter cone and on several cone segments were measured in place on this crater floor. Apical angles are 90° ± 5°, and P_s = 30 kb ± 5 kb in the area of these cones. Measurements show (a) that these shatter cones can be produced by shock waves interacting with free surfaces, (b) apices point in the direction of the originating energy source, (c) cone axes are normal to the shock wave front and pass through the center of the originating energy source. These data allow more confident use of shatter cones as criteria for shock wave deformation and direction of shock wave propagation at the larger natural impact or cryptoexplosion sites.

Mine Shaft (1969) Series.--In 1969 the Waterways Experiment Station, under the direction of the Defense Atomic Support Agency, detonated a 100-ton TNT sphere approximately tangent (buried 0.25 m with center 2.2 m above ground) to a hard rock surface (tonalite) at the Cedar City, Utah, test site. D. J. Roddy, with excellent cooperation from the crew of the U. S. Geological Survey Beaver aircraft, completed air blast, oblique and low altitude black and white, color and false-color IR stereo photography of the cratering experiment. The apparent crater, 19 m in diameter and 2.5 m deep, had a faulted, fractured uplift rim, an overturned flap over parts of the rim, and an irregular blocky ejecta blanket. After excavation, measurements of the true crater gave a diameter of 21.2 m and a depth of 4.2 m.

Blocks ejected from the crater and overlaying the crater rim were as large as 2 m across; one 25-ton block was ejected more than 70 m from ground zero. A survey of blocks ejected along the major rays showed masses as large as 27 kg at 615 m from the crater. One 225 kg block was ejected 440 m and formed a secondary crater 2 m in diameter. Terminal impact angles were measured where large blocks fell through Juniper trees; impact angles ranged from 45° to 83°.

Extensive secondary crater fields were formed in the sandy alluvial cover at average distances of between 100 to 150 m from the

main crater. These secondary craters were commonly elongated along radials to the main crater; many of the ejected blocks bounced several times to form more than one elongated secondary crater before coming to rest.

Geologic mapping and structural studies are still in progress.

PART C. COSMIC CHEMISTRY AND PETROLOGY

Chemistry of Cosmic and Related Materials (Contract R-66)

These investigative efforts have been devoted mainly to: (1) The refinement and/or development of microchemical techniques, particularly for the compositional analysis and characterization of small amounts of materials of astrogeologic interest. (2) Chemical investigations, research, and service in support of other branch acitivities in the fields of impact metamorphism, cratering, meteoritics, volcanology, geochemistry, and cosmochemistry. (3) Compositional analysis of 2 suites of returned lunar samples.

Distributive geochemical data for trace elements provide a direct measure of the equilibrium relations among coexisting minerals composing rock types. Such data are fundamental to a better understanding of genetic processes even where field studies are abundant and particularly in planetary exploration. Thus, a reasonable portion of this year's work focused on the distribution of trace elements between coexisting minerals.

Study of the distribution of Mn, Sc, and Co between coexisting biotite and hornblende from a large number of igneous rocks (Greenland, Gottfried, and Tilling, 1968; and Tilling, Greenland, and Gottfried, 1969) has been completed. These elements show an equilibrium distribution between biotite and hornblende but only the distribution of Mn appears to be temperature dependent; the distribution of both Mn and Sc exhibit some compositional dependence. The distribution of Sc has been studied further by analyzing a large number of coexisting minerals from the southern California batholith. This study shows that most of the minerals are in equilibrium with respect to Sc (magnetite is an exception) and that, contrary to common opinion, Sc is concentrated in residual magmas. A theoretical model for the distribution of trace elements between magma and crystals, which takes account of varying mineral abundances and distribution coefficients during crystallization, has also been developed (Greenland, L. P., accepted for publication by

American Mineralogist). Determination of crystal/liquid distribution coefficients of P has shown that P may be used to give a direct estimate of the fraction of liquid remaining during crystallization of a magma, (Anderson and Greenland, 1969). In connection with these distributive geochemical studies, analytical methods for the determination of Nb and Ge have been devised (Greenland and McLane, 1968).

Data concerning the distribution and abundances of siderophile elements can provide a better understanding of their fractionation in chondrites. Currently, work is in progress on methods for determining Ir; a non-destructive procedure involving triple coincidence counting appears to be satisfactory down to concentrations as low as 1 ppb Ir in a 1 gram sample; unfortunately, most rocks contain less Ir than this and the possibility of fire assay separation is being investigated to enable the determination of 0.00X ppb Ir.

The installation and operation of two new spectrographs was completed in anticipation of lunar work.

The Baird Eagle mount was upgraded from a coverage of approximately 1200A° in first order spectrography to a coverage of 2400A° by purchase of a new unit. The grating from the old instrument was transferred to the new spectrograph because of the desirable blaze for second order ultraviolet work.

A surplus Bausch and Lomb large Littrow prism spectrograph was positioned with the Baird grating, to permit simultaneous recording of alkali spectra on the B and L and ultraviolet spectra on the Baird. This will be used in the event of limited sample size.

Chemistry and Petrology of Apollo 11 Samples

Chemical analyses are being performed on two suites of typical lunar materials from Tranquility Base. The analyses and other descriptive information generated will be evaluated for their geochemical implications. The two suites, each consisting of 13 samples, total 34 grams of material representing three different rock types. The types are: (1) Crystalline, fine-grained, vesicular igneous rock-- sample # 10022; (2) Crystalline, coarser grained, vuggy microgabbroic rock-- sample # 10024; and (3) Breccia-- samples # 10046 and 10048. Also included is fine material composed of particles less than 1 mm in size from a core-- sample # 311079.

Using combined chemico - x-ray fluorescence techniques F. Cuttitta, E. Dwornik, and H. J. Rose are determining the abundances of 14 major elements (SiO_2, Al_2O_3, Fe_2O_3, FeO, MgO, CaO, Na_2O, K_2O, H_2O-, TiO_2, MnO, P_2O_5, Cr_2O_3, and ZrO_2) and 21 minor elements (Pb, Ag, Cu, Ga, Cs, Rb, Li, Mn, Cr, B, Co, Ni, Ba, Sr, V, Be, Nb, Sc, La, Y, and Zr). C. S. Annell and A. Helz are analyzing the same samples by emission spectroscopy.

Studies by E. C. T. Chao and O. B. James of Apollo 11 samples have been aimed at describing characteristic effects produced in the rocks by meteorite impact, and at determining the pre-shock characteristics of the rocks so that impact processes may be distinguished from those operative before impact. The unshocked samples were divided into two suites on the basis of texture, chemistry, and mineralogy, and a textural classification of the rocks of the dominant suite has been developed. Detailed studies of the compositions of the minerals of the unshocked rocks have been made with the electron microprobe.

Petrology of Meteorites
(Contract R-66)

Five penetration craters produced by the fall of stones of the Allende chondrite were mapped by D. P. Elston. The stones fell near Pueblo Allende on February 8, 1969, following the detonation of a brilliant fireball east of Hidalgo del Parral, Chihuahua, Mexico.

Allende stones characteristically are dense and tough. Those which produced the craters studied ranged in weight from about 8 kg to 35 kg. Two of the stones were recovered from their finders and both could be accurately positioned in their craters. The craters are asymmetric in cross-section, and typically have one crater wall with comparatively low-inclination and two to three steeply dipping to locally overhanging crater walls. Material ejected from the craters is characteristically deposited adjacent to the crater walls of low inclination.

The Allende fireball reportedly arrived from the southwest. The strewn field trends northeast, and is about 36 km long and 9 km wide (J. Hyde, personal communication, 1969). Large stones, weighing a few kg to more than 30 kg, were recovered in the northeast part of the field. Tiny meteorites, some as small as one gram, and completely enclosed by fusion crust, were recovered at the southwest end of the field (J. Hyde, personal cummunication, 1969).

Three of the penetration craters mapped occur in the north-central and northeasternmost part of the strewn field. The low-inclination walls, which dip southward approximately 25°, 35°, and 60°, are on the north; the steep walls, which dip approximately 83°, 98°, and 105°, are on the south. Ejecta are found on the north sides of the craters, adjacent to the crater walls with low inclination. In one crater the maximum angle of entry of the meteorite could be determined from both unbroken and broken overhanging branches of a bush; the penetration angle was approximately 70° or less, and the meteorite arrived from the north or northwest.

Two craters were mapped in the central and south-central parts of the field. Their low-inclination crater walls, which dip about 25° and 35° westward, occur on the east, and ejecta lay asymmetrically to the east. These meteorites appear to have arrived from the east or northeast.

The field data suggest that the stones arrived from directions that lay at large angles to the reported southwest to northeast path of the fireball. Moreover, the angles of penetration appear to have

been at some tens of degrees from the vertical, which is not compatible with the concept of fall of stones decelerated to free-fall velocities. The data suggest that the phenomena of fall and low velocity impact cratering by meteorites are not fully understood.

Cosmic Dust
(Contract R-66)

M. H. Carr continued his studies of high altitude airplane collections of debris from fireballs. Work on material from the Revelstoke fireball continued and a new set of filters were flown to collect debris from the Allende fireball and examined in detail. The Allende fireball of February 8, 1969, was observed over large areas of Texas, New Mexico and Arizona and resulted in a large meteorite strewn field near Parral, Mexico. Approximately 23 hours after the event filters were flown down-wind from the fall area at altitudes of 10,000 to 12,000 meters in an attempt to collect fireball material still remaining in the atmosphere.

Detailed examination of the filters revealed the presence of magnetite and siliceous spherules but in much smaller numbers than in the filters used for the Revelstoke event. The magnetite spherules were approximately twice as abundant as in background filters but within the expected range of background variations. The siliceous spherules were present in comparable numbers although none were found in the background filters. Virtually all the spherules were less than 10 μ in diameter, so that only semi-quantitative analyses were possible. The siliceous spherules are composed largely of Si and Fe with lesser amounts of Al, Mg, and Ca and traces of Na, K, and Ti. In addition to the spherical particles, a wide variety of irregular particles were collected but their chemistry could not be matched with the known chemistry of the fusion crust of the original meteorite and their origin is indeterminate.

In summary, very little particulate debris was collected in the atmosphere from the Allende fireball although many meteorites were found on the ground. The Allende event therefore differs markedly

from the Revelstoke event in which large amounts of material were found in the atmosphere but very little on the ground. Revelstoke and Allende are believed to typify two different kinds of events. In the Revelstoke type, the meteorite almost completely disintegrates in the atmosphere, generating a large infrasonic air wave, leaving large amounts of particulate debris in the atmosphere, and resulting in very few finds in the fall area. In the Allende type of event, the meteorite only partially breaks up, a much smaller air wave is generated, little particulate debris is left in the atmosphere, and most of the meteorite is deposited as cohesive fragments in the fall area.

PART D. GEOLOGIC SUPPORT FOR PLENETARY MISSIONS

Geochemical Requirements (Surveyor Chemistry) (Contract W-12,872)

E. D. Jackson and H. G. Wilshire interpreted preliminary alpha-scatter analyses from Surveyors V and VI as being compositionally similar to terrestrial tholeiite flood basalts, and an analysis of soil by Surveyor VII as being compositionally similar to terrestrial high-alumina basalt. Subsequent refinement of Surveyor V data revealed the high Ti, low alkali nature of mare materials from Mare Tranquillitatis as was further demonstrated by samples returned by Apollo 11, The alpha-scatter device is capable of distinguishing major geochemical provinces, and, when such data are interpreted in terms of geologic setting and photographic information, significantly narrows the choice of rock types represented by the analyses.

Geologic Exploration Strategy (Contract W-12,872)

M. H. Carr completed a document entitled Strategy for the Geologic Exploration of the Planets. It is being distributed as an Interagency Report: Astrogeology 19. The purpose of the document is to provide a guide to the orderly geologic exploration of the planets, to assign priorities to specific experiments, and to suggest areas where supporting Earth-based research can be most profitably pursued. The kinds of data that are most relevant to geologic interpretation are specified and the sequence in which data should be acquired is outlined. The document is intended as a supplement to previous more general documents and was written largely within the framework of recommendations of the Woods Hole Conference and the McDonald Committee on Space Research. A large number of Survey personnel contributed directly or indirectly to the report. The chapter on Stratigraphy and Structure was written largely on the basis of discussions with Z. S. Altshuler, J. F. McCauley and D. E. Wilhelms. The Cartography and Geodesy section summarizes recommendations from D. W. G. Arthur, R. M. Batson, W. T. Borgeson, A. P. Colvocoresses, and F. J. Doyle.

R. R. Doell, J. H. Healey, A. H. Lachenbruch, W. E. Lee, B. C. Raleigh, G. G. Schaber and Kenneth Watson contributed to the section in Geophysics and the Geochemistry section was written in collaboration with Priestly Toulmin and I. A. Breger. The strategy is based on current knowledge and is expected to require revision as our knowledge of the planets increases and as new analytical techniques develop.

Mars Mapping (Geologic Support for Mars Missions) (Contract W-12,872)

During the report period J. F. McCauley assessed the geologic significance of the Mariner 6 and 7 data and their implications concerning future exploration of Mars. Unfortunately only press release data and a preliminary report by Leighton, and others (1969) were available for study. In spite of their generally poor quality in terms of ground resolution, these data show clearly that Mars is a Moon-like object and that its surface is laterally heterogeneous-- as proven by the fact that at least four major terrain types can be recognized. The near-terminator region is photographable and craters as small as 3 km in diameter are identifiable in A camera pictures and 600 meter craters are identifiable with the B camera. Identification resolution for the A camera falls off to about 5 km at sun angles of 30°, and to 15 km at 60°. The effect of variation in lighting on system resolution will be studied further in order that subsequent imaging experiments such as those for 1971 and 1973 can be conducted to the best possible advantage.

The now demonstrable heterogeneity of Mars implies that the distribution pattern of surface units is important and that systematic photogeologic mapping will be an important exploration component. When enhanced Mariner 6 and 7 photographs become available several experimental Mars photogeologic maps will be prepared with a view toward adapting established lunar techniques for the Martian surface. However most, if not all of the A camera data are below the threshold of usability for photogeologic purposes

and is suitable mainly for crater size-frequency studies. The projected experimental maps will then have to be prepared from the B camera pictures which cover only a miniscule fraction of the surface and are non-contiguous.

Comparisons between the degree of cratering observed on Mars at resolutions of 0.1 km/TV line or 1 km/TV line (Mariners 6 and 7, A and B cameras) and different parts of the Moon have been started. Initial results indicate that in the 10 to 100 km size range Mars is somewhat less cratered than the most heavily cratered parts of the lunar terrae but clearly more cratered than the modified and younger terrae. These comparisons should be treated with caution because of the preliminary and incomplete nature of the data.

Refinement of the Mars surface model was initiated and preliminary results were transmitted by H. J. Moore to the Viking Mars 1973 project.

A proposal, solicited by NASA for the Viking Mars 73 Orbiter Imaging Science Team, was prepared and submitted by S. S. C. Wu. Orbital photography and photogrammetric data reduction are the main concern of this proposal. Besides the geodetic and photogrammetric applications as well as the geological interpretation, some suggestions regarding the selection and calibration of the camera were also offered in the proposal.

Analog Studies
(Contract W-12,872)

M. J. Grolier examined the feasibility of detecting aeolian features on Mars from spacecraft imagery. Wind activity has long been suspect on Mars because of the presence of an atmosphere and because of temporary obscurations of the surface by yellow clouds, widely interpreted as dust storms. In addition the wave of darkening, the filling of craters, and the rounding of surface features have all been interpreted as resulting from wind action. On the Earth, wind made forms are either depositional or erosional. The depositional forms include sand dunes, of silt and clay dunes, and accumulations of loess and volcanic ash. The erosional forms

consist of elongate grooves in the ground and the residual ridges between them (yardangs), desert valleys, desert hollows, and blow-outs. From the distribution and orientation of such aeolian landforms on Mars the wind regime over extended periods and over wide areas of the planet may be established. However, the laws governing the formation of these landforms on Earth are still imperfectly understood and their formulation is necessary before the laws can be appropriately scaled for the Martian conditions. The availability of Gemini photography of the Earth now enables aeolian landforms to be studies on a regional scale and will clarify the mechanics of their formation. Comparison of terrestrial photographs with those of Mars show that terrestrial aeolian features are not visible from photography with resolution similar to that presently available for Mars. However, some arcuate ridges on the southern polar cap of Mars may have formed as a result of wind action.

H. J. Moore lectured to Astronauts Alan Shepard, Ed Mitchell, and Joe Engle in Houston, Tex., and conducted them on a field study of craters near Flagstaff, Arizona. Both the lectures and the field study are designed to illustrate the use of fresh (young) lunar impact craters of progressively larger sizes to obtain samples from progressively deeper layers. Other lunar phenomena such as inverted stratigraphic sequences on crater rims, morphologic ages of craters, secondary impact craters, and boulder tracks were demonstrated.

Radar Evaluation
(Contract W-12,872)

During the contract year G. G. Schaber and R. E. Eggleton continued to evaluate the feasibility and anticipated geologic significance of spacecraft-borne bistatic and coherent side-looking radar experiments for mapping topographic, morphologic and other physical (including dielectric) properties of the surface of Venus.

The scientific and engineering need for such sophisticated unmanned spacecraft experiments has increased during recent months

owing to the second and third failures of Russian parachute probes (Venera 5 and 6) to successfully negotiate a functional soft landing on the hostile Cytherean surface. It appears more certain with time that spacecraft-borne radar mapping of the surface of Venus must be the initial step toward detailed geologic investigation of that planet.

Research into the geologic utility of Earth-based lunar and planetary delay-doppler radar techniques was greatly accelerated during the last funding year. Detailed geologic study of 70 cm (430 mhz) Earth-based lunar radar data (obtained from the Arecibo Ionospheric Observatory) of the Sinus Iridum quadrangle revealed excellent correlation between relative age of mare units and intensity of radar back-scatter. The lowest radar reflectivity values correlate well with the youngest mare units, which are characterized b low albedo, blue spectral reflectivity and relatively low crater densities. The regions of lowest diffuse radar reflectivity within the dark mare units are associated with partially flooded craters possibly indicating regions of most recent volcanic activity.

This continuing investigation indicates that Earth-based delay-doppler radar data can be of significant geologic value for Venus, Mars, and Mercury if resolution approaches that of current lunar data $(50\text{-}100 \text{ km})^2$. Present delay-doppler resolution on the Venus surface is still in the 100-200 km range, but indications are that significant improvements will be made in the next few years.

G. G. Schaber and R. E. Eggleton, were recently designated as investigators by NASA under a Jet Propulsion Laboratory CSM lunar radar sounding experiment now scheduled for Apollo flights 19 and 20. The 1.2 ghz (25 cm) calibration sensor proposed for the CSM experiment is similar equipment to that proposed by W. E. Brown, Jr. of Jet Propulsion Laboratory, for implementation on an unmanned Venus flyby and/or orbiting spacecraft in the 1975 period. It is anticipated therefore that geologic information obtained from the CSM lunar experiment would be invaluable in system designing and in interpreting data from later planetary radar experiments. The

second of several scheduled terrestrial overflights with the 1.2 ghz (25 cm) coherent, synthetic aperture radar system was accomplished in May of 1969. Many areas in the western United States sites were overflown, including, at Schaber's request, the area near Flagstaff, Arizona. The image data from this flight are now being evaluated.

Planetary Geodesy
(Contract W-12,872)

D. W. G. Arthur has been working on various geodetic problems that arise in photographing planets. He has made a general evaluation of the geodetic potentialities of the narrow angle cameras that are normally flown on planetary missions and, in addition, has made an evaluation of the geodetic utility of the Mariner 69 imagery. Bi-projective photogrammetry rests on the Fourcade Correspondence Theorem which asserts that the perspective cones associated with two photographs must be set so that each perspective ray in the first cone intersects the corresponding ray in the second in order to recover the original landscape form correctly. Fourcade showed that when the cones were placed so as to produce intersection for five pairs of rays it ensued automatically at all others. Fourcade's condition is necessary but not sufficient. The theorem breaks down in several cases, the most important for planetary work being the case when the angular fields are very small. The indeterminate element here is the dihedral angle between the two photo planes but this does not produce an insoluble problem in the mapping so long as the landscape is covered with photographs from two or more directions. The equations for the camera orientation are then applied to three or more overlapping photographs and the computed orientations imposed in the bi-projective mapping procedures.

If (x,y) are the photographic coordinates, the equations to be solved in a rigorous treatment are:

$$x = \frac{a(\xi - \bar{\xi}) + b(\eta - \bar{\eta}) + c(\zeta - \bar{\zeta})}{\ell(\xi - \bar{\xi}) + m(\eta - \bar{\eta}) + n(\zeta - \bar{\zeta})} \cdot Z$$

$$y = \frac{e(\xi - \bar{\xi}) + f(\eta - \bar{\eta}) + g(\zeta - \bar{\zeta})}{\ell(\xi - \bar{\xi}) + m(\eta - \bar{\eta}) + n(\zeta - \bar{\zeta})} \cdot Z$$

where Z is the effective focal length and

$$\Theta = \begin{pmatrix} a, & b, & c \\ e, & f, & g \\ i, & j, & k \end{pmatrix}$$

represents the rotation from the planetodetic system to the camera system. The unknowns are the elements a, b. . .k for each camera, the planetographic coordinates (ξ , η , ζ) for each surface point, and the planetodetic coordinates ($\bar{\zeta}$, $\bar{\eta}$, $\bar{\xi}$) of the spacecraft. The last must be derived from the tracking data using the longitude of the node ψ , the inclination of the planetary equator i, and the planet's rotation rate ω . Hence in general ψ , i, and ω are unknowns and their corrections must be present in the first order differential forms of the above equations.

For the i^{th} point measured on the k^{th} plate the observation reduces to

$$\Sigma_j \frac{\delta x_{ik}}{\zeta u_j} \cdot \delta u_j = (x_{ik\ abs.}) - x_{ik\ comp})$$

where u_j are the unknown parameters. To maintain orthogonality to the first order the orthogonal matrices are thrown into the form

$$\begin{pmatrix} a, & b, & c \\ e, & f, & g \\ \ell, & m, & n \end{pmatrix} \qquad \begin{pmatrix} 1, & \alpha, & \beta \\ -\alpha, & 1, & \lambda \\ -\beta, & -\alpha, & 1 \end{pmatrix}$$

but the postfactors are subsequently computed as rigorous orthogonal matrices using the elements α , β , λ .

Simple counts of unknowns and equations indicate values of about 20 for the number of points and number of plates.

Another failure situation arises if the spacecraft's orbit is a straight line through the center of the planet and the Mariner Mars 69 trajectories are such that they are in the neighborhood of this failure. At or near the straight line trajectory, the spacecraft positions and the planet can be rotated as one about the trajectory without violating the tracking data or the photographic measures. The solution therefore fails and the orientation of the plane's spin axis is indeterminate. Hyperbolae of high eccentricities such as followed by Mariners 6 and 7 are in practice not much better than a straight line trajectory so that accurate determination of the spin axis of Mars from the MM 69 imagery may be precluded.

Planetary Physics

In the course of Martian photometric investigations conducted with H. A. Pohn, R. L. Wildey developed a computerized procedure for determining interference filter parameters that enable an optimum match to a given magnitude-color system, such as the UBV system of Johnson and Morgan, when a sensor of arbitrary spectral response is employed.

R. L. Wildey, in collaboration with L. M. Trafton of the Air Force Weapons Laboratory, conducted an observational-theoretical investigation of the structure of the atmosphere of Jupiter. Using the 200-inch Hale telescope and a dual beam photometer employing a

Hg-doped germanium photoconductor, 41 approximately equatorial scans were obtained in the 9-13 μ band of the Jovian thermal spectrum. The scans were statistically analyzed, considering adjacent pixels (1/16 Jovian diameter) as independent, and a most probable scan for a zenith observation was synthesized. Probable error of pixels was well under one percent. For comparison, model atmospheres were constructed from which theoretical limb-darkening curves were derived. The models were "stellar" in that it was assumed that sunlight was absorbed well below the thermally opaque regions, so that a condition of constant net thermal flux was enforced at all overlying levels. Other scattering at thermal wavelengths was negligible, and the sources of opacity were the pressure-induced rotational and translational transitions in the external field-coupling of He-H_2 molecules and the discrete band absorptions of the vibration-rotation transitions of NH_3. A semi-theoretical model was assumed for departures from Lorentzian profile in the wing regions of the lines. The predicted limb-darkening underwent convolution with the spread functions describing both the finite photometer aperture and atmospheric seeing. The emergent specific intensity was also weighted by photometer spectral response. Both observational and theoretical limb darkenings were normalized to peak unity. The abscissa of the observational curve was then calibrated by equating the total area under the curve to that of the theoretical curve. In the resulting comparison it was found that the effective temperature is between 140 and 150°K, which implies Jupiter has an internal energy source 3 to 4 times larger than the solar energy it intercepts. Further work may lead to estimates of the helium to hydrogen ratio.

R. L. Wildey collaborated with D. N. Tompkins of Philco-Ford Corporation in the design of an imaging system suitable for deployment aboard a spin-stabilized spacecraft intended for missions to Jupiter. A spin-scan camera was designed with a variable polar angle driven by a cam to accommodate a given orbit. This allows high resolution with a line rate which still satisfied the Nyguist

criterion and the real-time bit rate of state-of-the-telemetry under the constraint imposed by spacecraft spin rate and Earth oriented spin vector. The camera employed a silicon PIN photodiode detector. Various modes of colorimetry, polarimetry, and grey-level number were incorporated on a variable multiplex basis to accommodate changes in range rate near encounter. The resulting configuration was estimated to weigh approximately 2 pounds and consume about one watt, housed in a cylindrical configuration 5 inches long and 4 inches in diameter. Resolution was about 0:02; frames were pan-Jovian, 6° wide.

R. L. Wildey investigated the problem of placing observational constraints on the structure of the Universe assuming the validity of the field equations of general relativity but without constraint of restriction on the metric tensor imposed by the Robertson-Walker line element, which assumes global homogeneity and isotropy. He concludes that unless results of computations of the mean density of the Universe can be raised a factor of 100, the observed log redshift apparent magnitude relation for cluster-galaxies only warrants the conclusion that the Universe is expanding <u>locally</u>. Its <u>global</u> behavior, which is the cosmological problem, is indeterminate due essentially to the infinity of geometric gravitation-inertia fields consistent with observations but due primarily to matter beyond the observational limit.

PART E. SPACE FLIGHT INVESTIGATIONS

Surveyor Television Investigations

(Contract WO-3027 terminated June 30, 1968; continued data reduction now funded under contract R-66.)

The new data on the physical characteristics of the lunar surface derived from the Surveyor pictures can be fitted to a simple ballistic model for the origin and development of the lunar regolith.

At a given locality, the size frequency distributions of craters on the lunar surface can be represented by two functions. Small craters follow a steady-state distribution of the form $F=\Phi c^{\mu}$, where F is the cumulative number of craters with a diameter equal to or larger than c, and c is the diameter of the craters and Φ and μ have the steady-state values $\Phi = 10^{10.9}$, $\mu = -2.00$ at all five Surveyor landing sites. Larger craters are represented by the function $F=\chi c^{\lambda}$, where $\lambda < \mu$ and χ varies from one landing site to another. The solution for c at the intersection of $F=\chi c^{\lambda}$ with $F=\Phi c^{\mu}$, designated as c_s, is the upper limiting crater diameter for the steady-state distribution. The value of c_s is a function of the age of the surface on which the regolith has formed.

The thickness of the lunar regolith may be estimated from a variety of observational data. The estimated thickness of the regolith at a given Surveyor landing site is bracketed by the original depths of (1) the smallest craters with blocky rims which cut through the regolith and excavate coherent material beneath, and (2) the largest, sharp, raised-rim craters without blocks which have been excavated wholly within the slightly cohesive material that forms the regolith.

Other direct estimates of the thickness of the regolith are the inferred original depth of the largest craters believed to have been formed by drainage of the regolith material into subregolith fissures and, at the Surveyor VII site, the depth at which the surface sampler instrument encountered coherent material. The thickest regolith was found at the Surveyor VI site,

where it is estimated to be more than 10 m thick, and the thinnest was found at the Surveyor VII site, where it is estimated to be 2 to 15 cm thick.

Particle counts from sample areas at each of the Surveyor landing sites show an approximately linear relationship between the log of the cumulative particle counts and the log of the particle size. A power function of the form $N=KD^{\lambda}$, where N is the cumulative number of particles with diameter equal to or larger than D and D is the diameter of particles, can be fitted to the data at each site.

The size-frequency distribution of resolvable fragments at the Surveyor III, V, and VI landing sites was found to be the same, within errors of estimation, but at the Surveyor I and VII sites coarse fragments are more numerous. Considering all five sites, a strong inverse correlation exists between the abundance of coarse blocks and thickness of the regolith. The coarsest fragments are most abundant at the sites with the thinnest regolith.

Mariner Mars 1971 TV Experiment
(Contract WO-8122)

During the past year, U.S. Geological Survey members of the MM 71 TV team (M. H. Carr, J. F. McCauley, D. J. Milton, and D. E. Wilhelms), led by H. Masursky, with both other TV team members and with other non-TV experimenters, have helped develop plans for two complementary Mars missions in order to best use the available spacecraft. Mission A will provide, by means of a Goldstone synchronous orbit, contiguous uniform resolution photography of as much as 70 percent of the planet for the chief purpose of defining regional stratigraphic and structural variations but also to provide a comprehensive framework for planning future missions. Mission B will concentrate on examination of variable surface features and the atmosphere by repeatedly photographing the same region at short time intervals

(possibly the same 3 regions every 4 days by means of a 4/3 Mars synchronous orbit). These developments are partially reported in a collectively written contribution by the Mariner 1971 experimenters that will appear in a forthcoming issue of Icarus.

In addition Survey personnel have participated in final hardware design and development of mission strategies and are currently active in planning procedures for mission operations and data processing.

Facsimile Camera Testing
(Contract WO-8122)

An evaluation of the metric properties of the facsimile camera system has been partly completed by J. D. Alderman. Study of this system was prompted by the availability of the "Houston Fax Camera" and by its potential application to the imaging of planetary bodies. Philco-Ford Corporation was contracted by NASA to refurbish the system, demonstrate performance with field tests, and define multiple characteristics such as photometric, photogrammetric, and colorimetric fidelity. The Branch of Astrogeologic Studies, U.S. Geological Survey, was assigned the position of observer and unofficial advisor to the contractor for the duration of field tests and undertook to evaluate the data obtained.

An indoor test range was built to Survey specifications and in addition the camera was field tested on a tuff flow at Camp Verde, Ariz., and on weathered granite at Granite Dells, Ariz. Imagery from the outdoor tests was sent to a number of geologists and engineers for evaluation. The concensus was that the stereo, vertical base, panoramic imagery effectively presents a scale related perspective view that is superior to frame photographic equivalents. The entire scene remains in continuous stereo offering easy and quick correlation of information content. The distraction of scene viewing rotated 90° is minor as viewer adaptation results quickly. The metric qualities of the camera are however less satisfactory. On the AP/C plotter,

S. S. C. Wu partially matched positive transparencies of 140° horizontal scans separated by a 30 in. vertical base. This base gives excellent stereo with very small scale changes allowing stereo viewing over the whole image without major adjustment of the instrument, but stereo viewing under high magnification (X15) is hindered by a screening effect due to line blending imperfections not removed by the facsimile reproducer. Additional destortions also result from the image reconstitution and these distortions prevented accurate photogrammetry in the test. Gross distortions could be removed by a computor driven, high precision X-Y plotter with high intensity variable light source and a variable aperture. Such a plotter could also provide image enhancement, color separations, scale changes, and fixed scale formats. Photometric fidelity results in additional problems, and the system is very unreliable photometrically with the present reconstitution method. Scans along a gray scale show a non-cyclic variance of unknown cause. Complete photometric analysis requires that the data be aquired in digital form and this is not available at this time. In general it was concluded that while the imagery from the fax camera is excellent for visual interpretation and has great photogrammetric potential, problems of image distortion and photometric non-reproducibility must be solved before the camera can be used effectively.